UC Irvine
UC Irvine Previously Published Works

Title

Strong canopy wind gusts across a topographic gradient and associated rainfall conditions in a Central Amazon forest

Permalink

https://escholarship.org/uc/item/4r92808w

Journal

Agricultural and Forest Meteorology, 391

ISSN

0168-1923

Authors

Emmert, Luciano
Trumbore, Susan
dos Santos, Joaquim
et al.

Publication Date

2026-12-01

DOI

10.1016/j.agrformet.2026.111504

Copyright Information

This work is made available under the terms of a Creative Commons Attribution License, available at https://creativecommons.org/licenses/by/4.0/

Peer reviewed

eScholarship.org Powered by the California Digital Library
University of California

Agricultural and Forest Meteorology 391 (2026) 111504

Contents lists available at ScienceDirect

Agricultural and Forest Meteorology

journal homepage: www.elsevier.com/locate/agrformet

Strong canopy wind gusts across a topographic gradient and associated rainfall conditions in a Central Amazon forest

Luciano Emmert [a,f], Susan Trumbore [b], Joaquim dos Santos [a], Adriana Simonetti [a], Adriano José Nogueira Lima [a], Niro Higuchi [a], Robinson Isaac Negrón-Juárez [c], Cléo Quaresma Dias-Júnior [d], Tarek El-Madany [b], Olaf Kolle [b], Gabriel Henrique Pires de Mello Ribeiro [e], Daniel Magnabosco Marra [f,b,*]

[a] National Institute of Amazonian Research, Forest Management Laboratory, Manaus, Amazonas, Postal Code: 69060-062, Brazil
[b] Max Planck Institute for Biogeochemistry, Biogeochemical Processes Department, Jena, Postal Code: 07745, Germany
[c] Lawrence Berkeley National Laboratory, Climate Sciences Department, Berkeley, California, Postal code: 94720, USA
[d] National Institute of Amazonian Research, Environmental Dynamics Coordination, Manaus, Amazonas, Postal Code: 69055-010, Brazil
[e] Federal University of Mato Grosso, Forest Engineer Department, Cuiabá, Mato Grosso, Postal Code: 78060-900, Brazil
[f] Julius Kühn Institute, Federal Research Centre for Cultivated Plants, Institute for Forest Protection, Quedlinburg, Postal Code: 06484, Germany

ARTICLE INFO

Keywords:
Wind gusts
Amazon forest
Topography
Rainfall
Convective systems

ABSTRACT

Wind disturbances shape forest structure and dynamics, yet direct observations of strong canopy wind gusts remain scarce. We developed a method to detect and characterize strong canopy wind gusts using 24 months (October 2021–September 2023) of high-frequency (1 Hz) meteorological measurements from an old-growth Central Amazon forest. Strong canopy wind gusts were defined as events with speed ≥10 m s^{-1}, representing the upper tail of the wind speed distribution and approaching speeds associated with tree snapping and uprooting in our study region. We identified 424 events, with maximum speeds reaching 17.9 m s^{-1} and durations up to 90 s. Events occurred on ~18% of observation days (~4% of total observation time), with 3.1 ± 2.9 (mean ± standard deviation) events day^{-1} and 17.2 ± 9.6 $month^{-1}$. Wind gusts were more frequent during daytime, although their intensity did not differ between day and night. Differences across the topographic gradient emerged at higher wind speeds, with the strongest and longest-lasting events occurring more frequently on elevated plateau. Gusts occurred year-round but were most frequent during the dry-to-wet transition (September–October). Significant relationships between rainfall intensity and gust frequency and duration emerged only during the most intense rainfall events, particularly above the 87th percentile (~40 mm h^{-1}). However, gusts commonly preceded heavy rainfall by 5–20 min, consistent with convective outflow processes and indicating spatial and temporal decoupling between wind and rainfall. These findings provide high-resolution, site-level insights into canopy wind variability and its links to local atmospheric and environmental conditions in tropical forests.

1. Introduction

Strong wind gusts, short-lived but high intensity wind events near and above the forest canopy, are often associated with convective processes linked to atmospheric instability in the Amazon (Nunes et al., 2016; Oliveira et al., 2026; Silva Dias, 2002). In this region, deep convection can produce intense downdrafts that, when they reach the surface, spread outward as downbursts, generating strong wind gusts (Bezerra et al., 2021; Garstang et al., 1998; Giangrande et al., 2023). The structure and dynamics of these events have been previously described, and classification frameworks proposed by Fujita (1981) and Wakimoto (1985) are commonly used to characterize downbursts according to their spatial extent (outflow diameter) – distinguishing microbursts (<4 km) from macrobursts (≥4 km) – and their association with precipitation – distinguishing between wet and dry downbursts depending on whether they are followed by intense rainfall (Fujita, 1985; Fujita and

* Corresponding author: Daniel Magnabosco Marra, Julius Kühn Institute - Federal Research Centre for Cultivated Plants, Institute for Forest Protection, Erwin-Baur-Str. 27, 06484, Quedlinburg, Germany
E-mail address: daniel.magnabosco@julius-kuehn.de (D.M. Marra).

https://doi.org/10.1016/j.agrformet.2026.111504
Received 13 January 2026; Received in revised form 22 August 2026; Accepted 28 September 2026
Available online 8 October 2026
0168-1923/© 2026 The Authors. Published by Elsevier B.V. This is an open access article under the CC BY license (http://creativecommons.org/licenses/by/4.0/).
Open access funding enabled and organized by Projekt DEAL.

Wakimoto, 1983).

In mid-latitude regions, gusts exceeding 25 m s^{-1} are typically classified as severe (Moller, 2001), whereas lower thresholds have been adopted in tropical environments. For example, Ferreira et al. (2026) used 15 m s^{-1} to characterize intense gusts in the Brazilian Amazon, reflecting regional atmospheric conditions and observed event distributions. Observations in the Central Amazon have shown that strong wind events closely associated with convective activity and intense rainfall are often preceded by rapid increases in wind speed ≥10 m s^{-1} measured at ~40 m height (Garstang et al., 1994; Greco et al., 1994).

Strong wind gusts can have important implications for forest ecosystems (Mitchell, 2013). In the Amazon, wind-related disturbances range from branch breakage and defoliation to treefall events affecting individual trees or clusters, and, in extreme and rare cases, large-scale windthrows that affect hundreds to thousands of hectares (Chambers et al., 2013; Negrón-Juárez et al., 2010; Nelson et al., 1994). These disturbances potentially shape forest structure and dynamics by influencing biomass stocks, carbon cycling, and species composition (Aleixo et al., 2019; Esquivel-Muelbert et al., 2020; Magnabosco Marra et al., 2018; Marra et al., 2014; Urquiza Muñoz et al., 2021). However, the disturbance magnitude depends on multiple interacting factors, including wind characteristics, storm structure, and forest properties such as canopy architecture and mechanical resistance (Belcher et al., 2012; Geitmann and Gril, 2018; Jackson et al., 2019; Quine et al., 2021; Ribeiro et al., 2016; Rifai et al., 2016; Ruel et al., 1998; van Emmerik et al., 2018).

Strong wind events may also influence forest–atmosphere exchanges in tropical forests. Previous studies have shown that dense tropical forest canopies frequently experience weak coupling between the subcanopy and the atmosphere above, affecting exchanges of CO_2, water vapor, ozone, heat, and momentum (Oliveira et al., 2018; Santana et al., 2018). Under these conditions, intermittent turbulence associated with stronger wind events may temporarily ventilate the canopy and enhance the transport of respired CO_2 and other scalars from the subcanopy to the atmosphere above (Gonçalves et al., 2024; Oliveira et al., 2018). Observations in Amazonian forests further indicate that strong wind events favor more coupled canopy-flow states and contribute substantially to nighttime sensible heat and momentum exchange (Mendonça et al., 2023). Turbulence generated above the canopy is often dissipated within the upper canopy layers, leaving the lower canopy relatively isolated from the atmosphere aloft and increasing the residence time of plant-emitted gases within the canopy (Freire et al., 2017; Santana et al., 2018). Consequently, understanding wind variability above and within the canopy is important not only for evaluating forest disturbance and tree mortality, but also for improving our understanding of canopy coupling and forest–atmosphere exchanges.

Seasonal patterns of strong wind gusts in the Amazon are expected to exhibit a pronounced annual cycle, as they are closely linked to the strong seasonality of convective activity in the region (Filho et al., 2015; Negrón-Juárez et al., 2017). This seasonal cycle is marked by frequent and widespread deep convection during the wet season and fewer but often intense convective systems during the dry and dry-to-wet transition periods (Nunes et al., 2016; Rehbein et al., 2018; Rehbein and Ambrizzi, 2023; Zhuang et al., 2017). Dry-to-wet season transition conditions are associated with enhanced lightning activity, stronger downdrafts, and more persistent cold pool dynamics (Albrecht et al., 2011; Giangrande et al., 2023; Oliveira et al., 2026; Williams et al., 2002), which indicate atmospheric environments conducive to more vigorous storm development (Gora et al., 2025). Such conditions may favor more intense wind gusts during specific periods of the year (Ferreira et al., 2026).

At local scales, the interaction between wind and the forest surface is governed by environmental and structural controls (Gardiner et al., 2019). Topography influences wind exposure, flow acceleration, and turbulence, with elevated and exposed terrain generally experiencing stronger winds than sheltered areas such as slopes and valleys (Belcher et al., 2012; Ruel et al., 1998). In the Central Amazon, landscapes composed of plateaus, slopes, and valleys are widespread (Rennó et al., 2008), yet their influence on canopy-level wind regimes remains insufficiently quantified.

Most current knowledge of wind disturbances in the Amazon is derived from indirect observations, including field-based assessments of damage, remote sensing analyses, and reanalysis datasets (Emmert et al., 2023; Marra et al., 2014; Negron-Juarez et al., 2023; Negrón-Juárez et al., 2017, 2018). While these approaches provide valuable regional-scale insights, they have limited ability to resolve short-duration wind gusts and characterize their variability at fine spatial scales, particularly across heterogeneous terrain with subtle topographic gradients (Davidson and Millstein, 2022; Minola et al., 2020; Wang and Chen, 2025). Remote sensing typically captures the consequences of wind events rather than the events themselves, and reanalysis products rely on temporally averaged fields that do not resolve gust-scale variability (Harris et al., 2020; Hersbach et al., 2020; Huffman et al., 2020; Schmitt et al., 2023). This limitation is especially relevant in tropical forests, where wind gusts are highly localized and transient (Gonçalves et al., 2024; Oliveira et al., 2026).

Understanding these processes is particularly important given ongoing and future climate change. Recent studies suggest that convective activity and extreme precipitation is intensifying in the Amazon, with predictions for altered future wind regimes and increases in the likelihood of wind-associated disturbance events (Feng et al., 2023; Urquiza-Muñoz et al., 2024). Given the sensitivity of tropical forests to altered disturbance regimes and their role in the global carbon cycle, improving process-based understanding of strong wind gusts is essential (Brando et al., 2025; Flores et al., 2024).

Here, we investigate strong wind gusts measured at canopy height (hereafter, strong canopy wind gusts) across a topographic gradient and rainfall conditions in a Central Amazon forest located within a hotspot of large (≥30 ha) windthrow events in the Amazon Basin (Urquiza-Muñoz et al., 2024). We propose a framework to identify and characterize these wind gusts by using high-frequency (1 Hz) wind measurements collected over a 24-month period. Specifically, we address the following questions: (i) What are the main characteristics of strong canopy wind gusts in terms of frequency, intensity, and duration? (ii) How do these characteristics vary across topographic positions? and (iii) How are these events associated with rainfall conditions?

2. Material and methods

2.1. Study area

Our study was conducted in an old-growth *terra-firme* forest in Central Amazon, located ~100 km north of Manaus, Brazil, at the Tropical Silvicultural Experiment Station (EEST, coordinates 2°38′16"S/ 60°11′39"W) of the National Institute for Amazonian Research (INPA) (Fig. 1b). Our study is part of the INVENTA project (i.e., Wind-Tree Interactions in the Amazon, *Interação Vento-Árvore na Amazônia* [Portuguese]; Marra et al., 2018; Simonetti et al., 2023), which aims at integrating research on tree architecture and biomechanics with atmospheric and biogeochemical processes influencing forest dynamics and carbon balance. INVENTA includes an 18-ha permanent plot established in 2000 (Pinto et al., 2003), covering the topographic variation typical of *terra-firme* forests in the Central Amazon. The site's elevation above the canopy surface ranges from 67 – 145 m above sea level (Fig. 1c), with an undulating relief consisting of plateaus, steep slopes and narrow valleys associated with perennial drainages (Ferraz et al., 1998; Rennó et al., 2008). Canopy disturbances associated with wind across the entire plot (18 ha) were also monitored monthly using drone-based RGB-photogrammetry (Simonetti et al., 2023).

The *terra-firme* forest is the most common forest type in the Amazon basin (Braga, 1979) and is characterized by a continuous canopy, dense understory and high diversity – up to more than 280 tree species (≥10

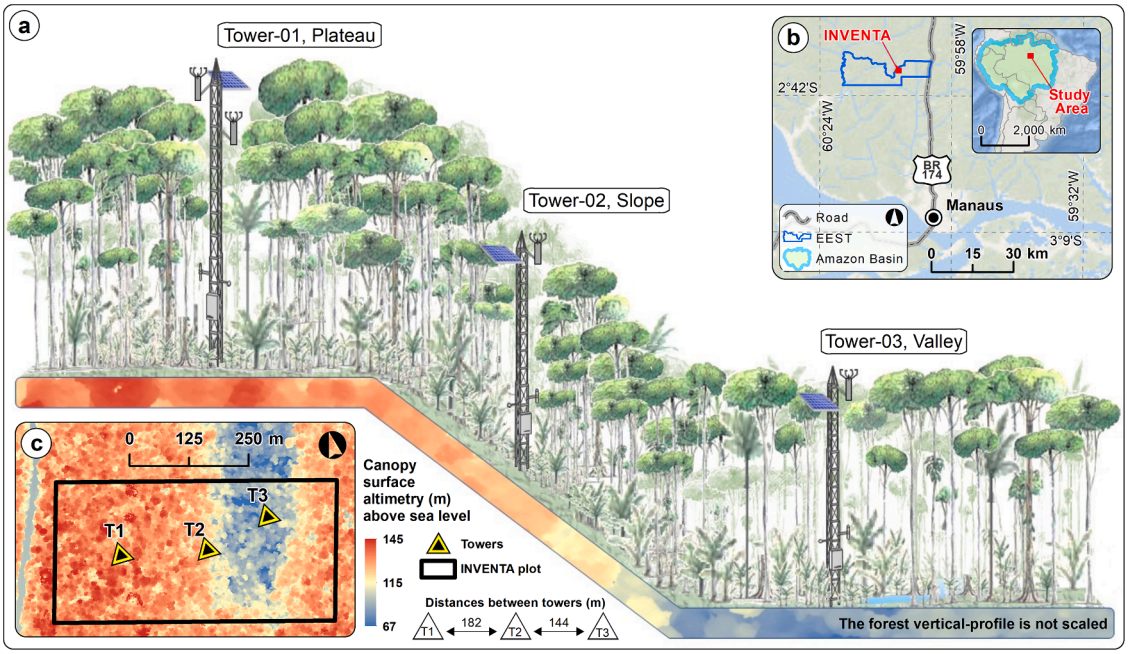


Fig. 1. Location and design of the INVENTA plot and tower infrastructure. (a) Schematic profile of the meteorological towers across the topographic gradient. (b) Location of the EEST and INVENTA project. (c) Digital surface model generated from drone imagery, representing the canopy surface altimetry relative to sea level and the locations of the towers within the 18-ha permanent plot.

cm DBH) can occur in a single hectare (De Oliveira et al., 1999). The study plot is covered by an old-growth *terra-firme* forest with closed canopy, tree density of 623 ± 66 trees ha^{-1} and height 28.65 ± 0.46 m (mean ± standard deviation) for trees ≥10 cm DBH (Araújo, 2019; Carneiro, 2004; Lima, 2010; Pinto et al., 2003). The INVENTA plot and the contiguous forest have remained free from significant human or natural disturbances for at least 60 years.

The soils on the plateaus have high clay content, transitioning to sandy soils in the valleys, which can be seasonally flooded (Chauvel et al., 1987; Ferraz et al., 1998; Luizão and Schubart, 1987). In general, these soils have relatively low fertility, low pH, low phosphorus availability, high aluminum concentration, and low organic carbon content (Cunha et al., 2022; Telles et al., 2003).

The climate in the region is classified as tropical monsoon (*Am*) according to the Köppen-Geiger system, with distinct dry and rainy seasons (Peel et al., 2007). The rainy season lasts from December to May, while the dry season extends from June to November, with a pronounced dry period between July to September, during which monthly precipitation is typically below 100 mm (Marengo et al., 2001; Sombroek, 2001). The mean temperature and annual precipitation recorded in our study site were 26.2 ± 3.2° C and 2,304.1 ± 50.3 mm (mean ± standard deviation from 2021-2023), respectively (Fig. S1).

2.2. Acquisition of meteorological data

Within the INVENTA plot, we installed three triangular towers in topographic positions representing plateau, slope, and valley, aligned parallel to the prevailing east–west wind direction in the region (Tóta et al., 2012), Fig. 1a), and covering an elevation range of ~70 m (Fig. 1c). The plateau tower (T1) is 36 m tall and equipped with two 2D sonic anemometers installed at heights of 33 m and 36 m. T1 is also instrumented with a tipping-bucket rain gauge, a temperature-humidity sensor, and a pressure transmitter (see details on instruments in the Supplement Material, Fig. S2). These instruments were installed at ~33 m height to capture meteorological conditions close to the canopy. The slope and valley towers (T2 and T3, respectively) are both 33 m tall and equipped with a single 2D sonic anemometer installed at 33 m height. In this study, we used only wind data collected at 33 m above local ground level, allowing for direct comparison among the three towers.

All towers are equipped with a datalogger (CR6, Campbell Scientific) that records, preprocesses and stores the data. Instruments and dataloggers are powered by a solar energy system. All instruments record data continuously at a frequency of 1 Hz. In this study, we used wind data from all three towers and rainfall data from the rain gauge at T1. Because only one gauge was operated, rainfall variability within the INVENTA tower network itself was not directly measured. Given the short distance between towers (~160 m), we assumed limited rainfall variability across the study area at this spatial scale, an assumption also supported by repeated field observations during maintenance campaigns, though it could not be directly quantified. Direct evidence on rainfall variability at such short distances in tropical forests remains scarce; as indirect support, observations from two towers at the ATTO site (~150 km from the INVENTA area, Andreae et al., 2015), separated by ~640 m, showed highly similar rainfall temporal patterns and magnitudes during most precipitation events, with differences typically within ~5 mm day^{-1}. While this comparison from a nearby but distinct site does not replace direct measurements at INVENTA, it lends indirect support to the use of a single rain gauge as reasonably representative of local rainfall conditions for most events. Localized variability may nonetheless occur during isolated convective storms, particularly for short-duration rainfall events.

The anemometer data are stored at raw frequency (i.e., 1 Hz), while the rainfall data are preprocessed and stored as total rainfall volume at 5-minute intervals. The towers were built in September 2019, and the instrumentation was completed by March 2020. Data have been collected continuously since then, but here we analyzed data collected between 01 October 2021 and 30 September 2023.

Meteorological time-series data can be affected by instrument malfunctions, external influences, and recording errors (Faybishenko et al., 2022). To minimize these potential non-sampling errors, we performed the data quality-control protocol described by Zahn et al (2016). This protocol includes visual graphical analysis of the data time series to identify patterns and inconsistencies, as well as error-handling methods such as missing value imputation and flagging, identification and

removal of impossible or implausible values through bounds testing, and elimination of random electronic spikes (Mauder et al., 2013; Rollenbeck et al., 2016; Vickers and Mahrt, 1997).

2.3. Data analysis

2.3.1. Defining strong canopy wind gusts

We adopted the definition of a gust as a sudden, relatively large increase in wind speed, quantified as increased deviations from the mean (Kristensen et al., 1991). Only gust events with a minimum total duration of three seconds (Harper et al., 2010), including the acceleration and recovery phases before returning to conditions similar to the pre-gust mean speed, were considered (Beljaars, 1987; Gomes and Vickery, 1978; Kantz et al., 2004; Kristensen et al., 1991; Mitsuta and Tsukamoto, 1989). The duration during which wind speed exceeded the selected threshold was analyzed separately.

Among detected gusts, we defined strong canopy wind gusts as those reaching a minimum speed of 10 m s^{-1}. This threshold was selected based on the statistical distribution of wind speeds in our dataset, where values above 10 m s^{-1} correspond to the upper tail (99.998th percentile) of all wind speed observations. These events are relatively infrequent and high-intensity (Fig. S3a-b). Wind speeds within this range near canopy height (~40 m) have also been reported as precursors to downburst conditions (Ferreira et al., 2026; Garstang et al., 1998; Greco et al., 1994), and forest disturbance-related processes in the Amazon (Negrón-Juárez et al., 2017, 2010).

In addition, mechanical stability analyses performed on 60 canopy trees in a forest contiguous to the INVENTA plot identified 10.75 m s^{-1} as the minimum wind speed associated with potential tree mechanical failure (Peterson et al., 2019; Ribeiro et al., 2016). The threshold adopted in this study (10 m s^{-1}) is therefore close to this empirically derived value, while also allowing a sufficient number of events for robust statistical analysis. Although wind speeds within this range may be associated with increased susceptibility to mechanical stress, the occurrence of actual tree damage depends on multiple interacting factors, including storm characteristics and forest structure (Gardiner, 2021; Quine et al., 2021). Therefore, the 10 m s^{-1} threshold was used here as an operational criterion to identify high-intensity wind gusts associated with atmospheric conditions conducive to canopy disturbance, rather than as a direct indicator of tree damage.

To identify and characterize strong canopy wind gusts, we developed a three-step framework to calculate three attributes: maximum speed, mean direction, and strong-gust duration (i.e., the time during which wind speed remains continuously ≥10 m s^{-1}) (Fig. 2). First, to select the gust of interest, we focused on those that exceeded the minimum threshold of wind speed of 1.85 m s^{-1}, which was based on the mean plus one standard deviation (1.06 m s^{-1} + 0.79 m s^{-1}) observed over the 24-month measurement period. Using one standard deviation allowed us to reliably select gusts that exceeded the typical wind speed observed just above the canopy (~1 m s^{-1} at 35-55 m height) reported for the region (Andreae et al., 2015; De Santana et al., 2017; Garstang et al., 1998; Tóta et al., 2012) (Fig. 2a).

Second, the time between the onset of the gust and return to the minimum threshold of 1.85 m s^{-1} was defined as the total duration. Only gusts with a minimum total duration of three seconds were retained, following the definition of wind gusts adopted by the World Meteorological Organization (Harper et al., 2010). Gusts separated by more than three seconds were considered independent events. For each event, we recorded the maximum wind speed and mean wind direction (Fig. 2b).

Third, from each gust, we computed the strong-gust duration as the time during which wind speed remained ≥10 m s^{-1} (Fig. 2c). Therefore, a strong canopy wind gust was defined as a gust with a minimum total duration of three seconds and a minimum strong-gust duration of one second.

2.3.2. Relating strong canopy wind gusts and meteorological variables

Our analyses showed that strong-gust duration explained 70% of the variation in maximum speed, compared to only 6% explained by total duration (Text S1 and Fig. S4). This indicates that strong-gust duration (time with wind speed sustained ≥10 m s^{-1}) is more closely associated with the intensity of wind events, whereas total duration includes extended periods of lower wind speeds with limited tree disturbance relevance (i.e., wind speeds close to the 1.85 m s^{-1} threshold). This result is consistent with experimental studies examining tree responses to wind loading under controlled conditions (England, 2000; Gardiner, 2021; Holmes et al., 2014; Moore and Maguire, 2004; Quine et al., 2021), which emphasize the importance of sustained high wind speeds in determining mechanical stress on trees. Based on this evidence, our subsequent analyses focused on the following key attributes: number of strong canopy wind gusts, maximum wind speed, mean wind direction, and strong-gust duration. For clarity and to optimize figure layout, these variables are referred to as "Max speed" and "Duration" in the figure axes presented in the Results section.

We summarized the selected attributes of strong canopy wind gusts,

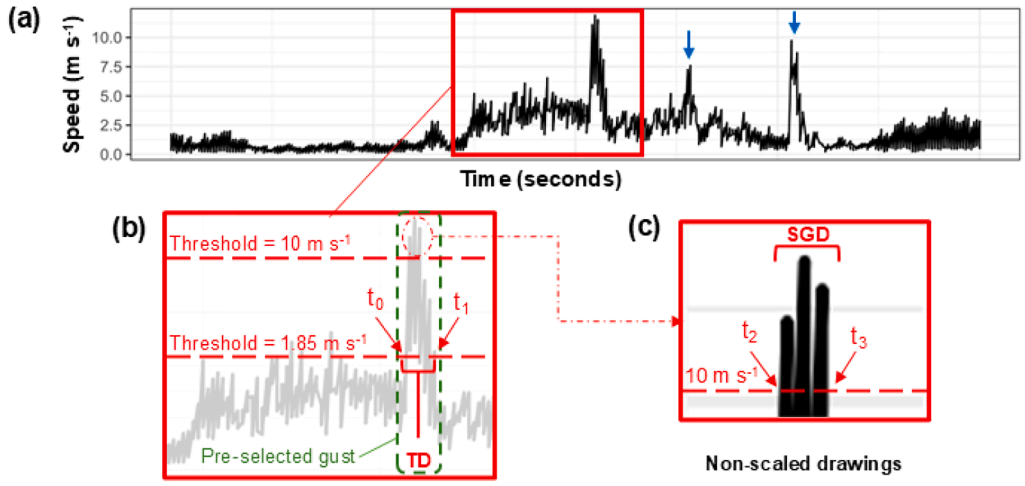


Fig. 2. Schematic representation of the framework of identifying strong canopy wind gusts. (a) Example of wind speed time series where strong canopy wind gusts were identified. In this panel, other gusts indicated by the blue arrows were not included because they did not exceed 10 m s^{-1} for 3 seconds; (b) Gusts exceeding a minimum threshold of 1.85 m s^{-1} and reaching or exceeding 10 m s^{-1} were pre-selected. The start (t_0) and end (t_1) times of the gusts were recorded, and total duration (TD) was computed as the time interval from t_0 to t_1; (c) From the pre-selected gusts, strong-gust duration (SGD) was computed as the time from t_2 to t_3, representing the period which the gust sustained speeds ≥10 m s^{-1}. Threshold lines in panels (b) and (c) were not scaled to improve clarity.

originally recorded at 1 Hz, to a 5-minute temporal resolution to match the 5-minute rainfall data. We analyzed the data separately for each topographic position (i.e., plateau, slope, and valley). We also evaluated potential differences according to time of day (day: 06:00–17:59; night: 18:00–05:59, local time) and season (dry: June to November; wet: December to May).

2.3.3. Statistical analysis

All statistical analyses were performed in R 4.5 (R Core Team, 2025), adopting a probability level of 95%. We tested the normality and variance homogeneity of the data by the Shapiro-Wilk and Levene-Brown-Forsythe tests using *RVAideMemoire* and *onewaytests* packages, respectively (Dag et al., 2018; Herve, 2023). As the data showed non-normal distributions and heterogeneous variances, non-parametric methods were applied, and medians were used as measures of central tendency (Gotelli and Ellisson, 2013).

To address the first research question, concerning the main characteristics of strong canopy wind gusts, we evaluated differences in gust attributes between daytime and nighttime periods using the Mann–Whitney–Wilcoxon test implemented in the *rstatix* package (Kassambara, 2023). To address the second research question, regarding the influence of topography, we assessed differences in gust attributes among plateau, slope, and valley positions using the Kruskal–Wallis test implemented in the *stats* package (R Core Team, 2025), followed by Dunn test with Bonferroni correction for pairwise comparisons using the *FSA* package (Ogle et al., 2023).

To address the third research question, related to the association between rainfall and wind gust characteristics, we applied cross-correlation analysis (Zebende, 2011) between rainfall rate (mm h^{-1}; predictor variable) and wind gust attributes (response variables) using the *forecast* package (Hyndman et al., 2024). This approach accounts for potential time lags between rainfall and wind responses (Kristoufek, 2014; Podobnik and Stanley, 2008), which are common in non-stationary atmospheric processes (Barry and Chorley, 2003; Dunlop, 2017) involving complex changes that do not necessarily occur concurrently among variables (de Oliveira Santos et al., 2012; dos Anjos et al., 2015; Kavasseri and Nagarajan, 2004; Koçak, 2009). Positive lags indicate that variations in wind attributes precede changes in rainfall, whereas negative lags indicate the opposite, and zero lag indicates synchronous variation. Correlations were evaluated within a ±2-hour window around each event. The time lag associated with the maximum correlation was then used to align rainfall and wind data using the *DataCombine* package (Gandrud, 2016).

Following this alignment, we quantified the relationships among log-transformed wind gust attributes (number of events, maximum speed, and strong-gust duration) and rainfall rate using linear models of the form $\log(y + 1) \sim \log(x + 1)$. Separate models were fitted for each pair of predictor and response variables across rainfall percentiles (0th–99th), allowing the evaluation of how relationships vary with rainfall intensity. For each model, we calculated the Pearson correlation coefficient (r), adjusted coefficient of determination (R^2), and p-value using the *stats* package. Higher values of r and R^2, together with lower p-values, were used to identify rainfall conditions under which the strongest relationships occurred.

3. Results

3.1. Characteristics of strong canopy wind gusts

We analyzed 17,348 hours of wind data, of which approximately 4% contained strong canopy wind gusts. These events were recorded in all months of the study period but occurred on only 133 (~18%) of the 730 analyzed days. In total, 424 events were identified during the 24-month measurement period. On days with events, the mean number of gusts was 3.1 ± 2.9 (mean ± standard deviation), corresponding to a monthly average of 17.2 ± 9.6 events. The number of events was similar between the two annual periods, with 213 events recorded from October 2021 to September 2022 and 211 from October 2022 to September 2023. Maximum wind speed ranged from 10 to 17.9 m s^{-1}, while strong-gust duration ranged from 1 to 90 s (Table 1).

Most events occurred during daytime, accounting for 363 (85.6%) of the total, whereas 61 events (14.4%) were recorded at night (Fig. 3a). Despite this difference in frequency, no significant differences were detected between daytime and nighttime medians of wind speed ($p = 0.83$) or strong-gust duration ($p = 0.41$) (Fig. 3d-e; Table 1). The highest values of wind speed and strong-gust duration were observed during daytime hours, particularly between 10:00 and 16:00 local time (Fig. 3a-c). However, variability in both attributes remained high throughout the daily cycle.

3.2. Variation across topographic positions

Of the 424 strong canopy wind gusts identified during the study period, 302 were recorded at the plateau, 98 at the slope, and 24 at the valley (Fig. 4a). These values represent tower-specific detections and may include simultaneous observations of the same atmospheric event across multiple towers, reflecting local variability in wind conditions within the study area.

Despite differences in the number of detected events, median wind speed did not differ significantly among the three topographic positions ($p > 0.05$ all, Fig. 4a; Table 1). In contrast, strong-gust duration differed among positions, with higher median values at the plateau. Pairwise comparisons indicated significant differences between plateau and slope ($p = 0.03$) and between plateau and valley ($p = 0.02$), whereas slope and valley did not differ ($p = 0.18$) (Fig. 4b; Table 1).

Further insight into these patterns is provided by events recorded simultaneously across towers. Differences among topographic positions were more evident in the upper range of the distributions, particularly at the plateau. A total of 29 events (~7% of the total) were recorded almost simultaneously (≤30 s difference) at two or more towers. Among these, 25 events (86%) recorded higher wind speed and longer strong-gust duration at the plateau compared to lower positions. All simultaneous events had wind speeds ≥10.8 m s^{-1}, corresponding to the upper half of the wind speed distribution (Fig. S3a). Maximum values of wind speed and strong-gust duration also decreased from plateau to valley (Table 1).

Wind direction also varied among tower locations. At the plateau and slope, wind gusts were predominantly from easterly directions, with mean azimuths of 100° and 93.6°, respectively (Fig. 4c-d). In contrast, at the valley, wind direction during strong gusts was predominantly from the south to southeast sector, with a mean azimuth of 161.6°, consistent with the orientation of the local topographic gradient (Fig. 4e; Fig. 1c).

3.3. Association with rainfall conditions

Strong canopy wind gusts occurred more frequently during the dry season, with 249 detected events compared to 175 events in the wet season (Fig. 5a). Median strong-gust duration did not differ significantly between seasons ($p = 0.14$, Fig. 5c; Table 1), whereas median wind speed was higher during the dry season ($p = 0.05$, Fig. 5b; Table 1). The highest values of wind speed and strong-gust duration were recorded during the dry season (Table 1), consistent with the upper range of the distributions.

At the monthly scale, the frequency and characteristics of events showed marked variability over the study period, with a peak in July ($n = 73$, Fig. 5d). Maximum wind speed and strong-gust duration were higher during the transition from the dry to the wet season, particularly in September and October (Figure 5Fig. 5e-f).

Seasonal variations in wind direction were also observed. Strong canopy wind gusts were predominantly from the eastern sector in both seasons (Fig. 6a-b), with a tendency toward the southeast sector during the dry season and toward the northeast sector during the wet season. Monthly variability in wind direction was more pronounced during

Table 1
Descriptive statistics of strong canopy wind gusts recorded at the INVENTA platform from October 2021 to September 2023. Wind speed and strong-gust duration are summarized by minimum (Min), maximum (Max), and median values. Letters indicate results of non-parametric tests comparing medians among groups: Mann–Whitney–Wilcoxon test for daytime period comparisons and Kruskal–Wallis followed by Dunn test with Bonferroni correction for topographic position and seasonal comparisons. Equal letters indicate no significant differences, whereas different letters indicate statistically significant differences ($p < 0.05$).

Category		Number of events	Wind Speed (m s^{-1})			Strong-gust duration (s)		
			Min	Max	Median	Min	Max	Median
Topographic Position	Plateau	302	10	17.9	11.1 (a)	1	90	3 (a)
	Slope	98	10	16.2	10.9 (a)	1	30	2 (b)
	Valley	24	10.1	13.5	10.7 (a)	1	16	1 (b)
Daytime period	Day	363	10	17.9	11 (a)	1	90	2 (a)
	Night	61	10	14.7	11.1 (a)	1	30	2 (a)
Season	Dry	249	10	17.9	11.1 (a)	1	90	3 (a)
	Wet	175	10	14.8	10.9 (a)	1	30	2 (a)

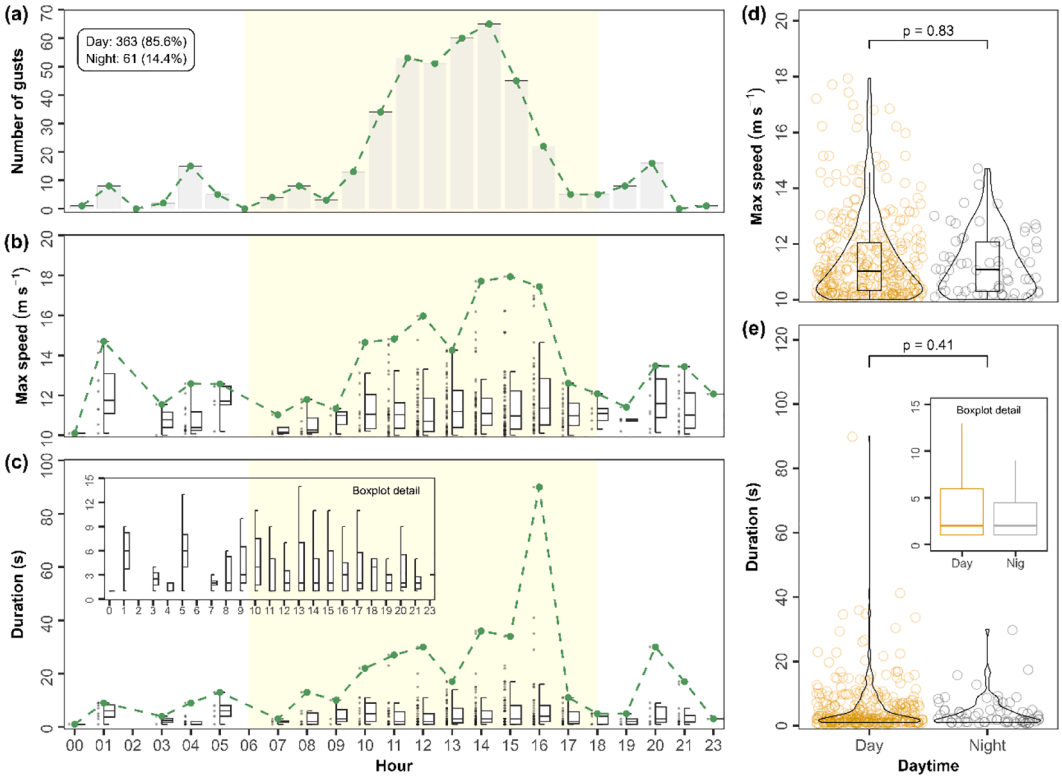


Fig. 3. Diurnal patterns of strong canopy wind gust attributes over the 24-month measurement period.
(a) Number of detected events by hour of day, with inset values indicating the proportion of events occurring during daytime and nighttime; (b) Maximum wind speed (m s^{-1}) and (c) Strong-gust duration (s), with boxplots representing the distribution of values within each hourly bin and dashed lines indicating median values; the inset in (c) provides a detailed view of the distributions to facilitate visualization of central tendencies; (d) Maximum wind speed and (e) strong-gust duration compared between daytime and nighttime periods, with p-values from Mann–Whitney–Wilcoxon tests; the inset in (e) shows boxplots highlighting the distribution of duration values. Shaded areas indicate daytime (06:00–18:00). The y-axis label "Duration (s)" in panels (c) and (e) refers to strong-gust duration (the period during which the gust maintains a wind speed of ≥10 m s^{-1}). All attributes were calculated using tower-specific detections without distinguishing among topographic positions. In panels (a), (b), and (c), the maximum values of attributes recorded per hour are represented by green points connected by dashed green lines.

transitional months, particularly in May and October (Fig. 6c).

Cross-correlation analysis indicated that the strongest relationships between rainfall rate (mm h^{-1}) and wind gust attributes occurred at a lag of +5 minutes for the number of events and strong-gust duration (Fig. 7a and c), indicating that increases in these attributes tended to precede rainfall. In contrast, no significant relationship was observed for maximum wind speed (Fig. 7b. Consistent with this pattern, most events (n = 291; 68.8%) were recorded at least 5 minutes prior to rainfall, whereas the remaining events (n = 133; 31.3%) did not show a clear temporal association with rainfall occurrence. No significant correlations were observed at longer lags (e.g., 20 minutes), indicating that the relationship between wind gusts and rainfall is primarily restricted to short timescales.

Rainfall rate was positively associated with the number of events and strong-gust duration at the event scale (Fig. 7d and f), although these relationships were weak ($R^2 = 0.05$ and 0.02, respectively). In contrast, no significant relationship was observed between rainfall rate and maximum wind speed ($R^2 = 0.01$, $p = 0.1$; Fig. 7e). Across rainfall percentiles, the strength of the relationships varied among attributes (Fig. 7g-i). For the number of events and strong-gust duration, both the Pearson correlation coefficient (r) and the coefficient of determination (R^2) increased with rainfall intensity, with the strongest relationships observed near the upper end of the distribution. In contrast, the relationship between rainfall rate and maximum wind speed remained weak and non-significant across percentiles. The strongest associations were identified at the 87th percentile (rainfall rate ~40 mm h^{-1}). At this level,

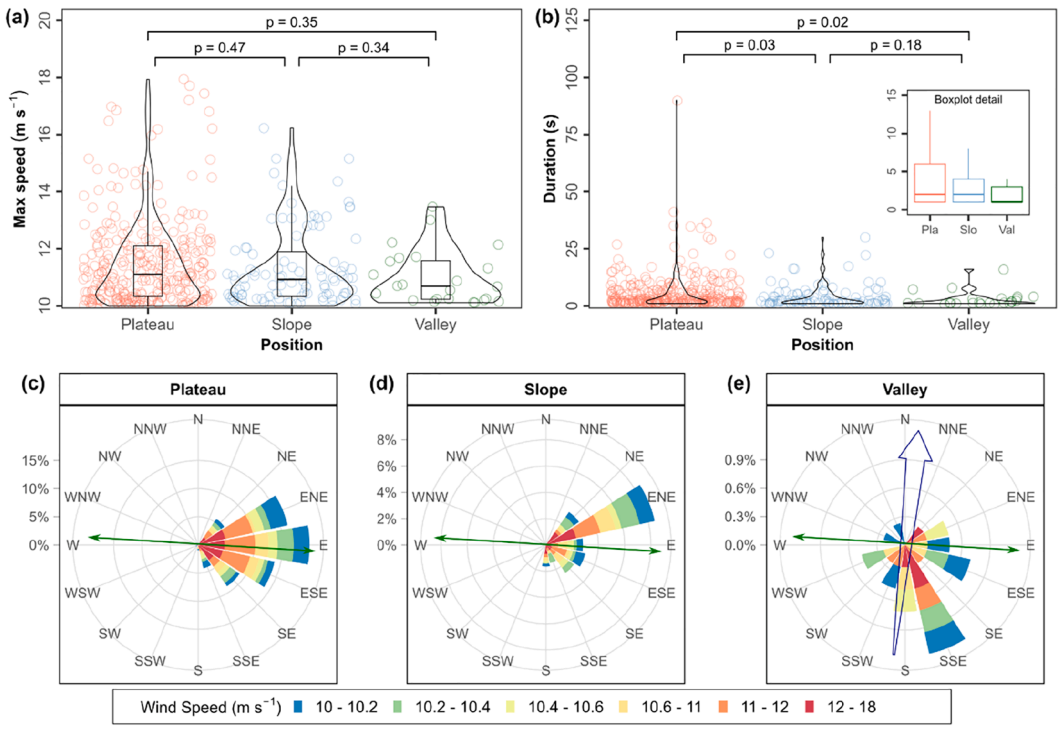


Fig. 4. Variation in strong canopy wind gust attributes across tower locations along the topographic gradient. (a) Maximum wind speed (m s^{-1}); (b) Strong-gust duration (s); (c) Wind direction at the plateau; (d) Wind direction at the slope; and (e) Wind direction at the valley. In panels (a) and (b), p-values from Dunn–Bonferroni post hoc tests are shown above the brackets. In panels (c)–(e), the radial axis represents the frequency (%) of events by wind speed classes. Green arrows indicate the alignment of the towers in panels (c)–(e), and the blue arrow in panel (e) indicates the orientation of the valley in the vicinity of the towers, following the local topographic gradient from the headwater downslope.

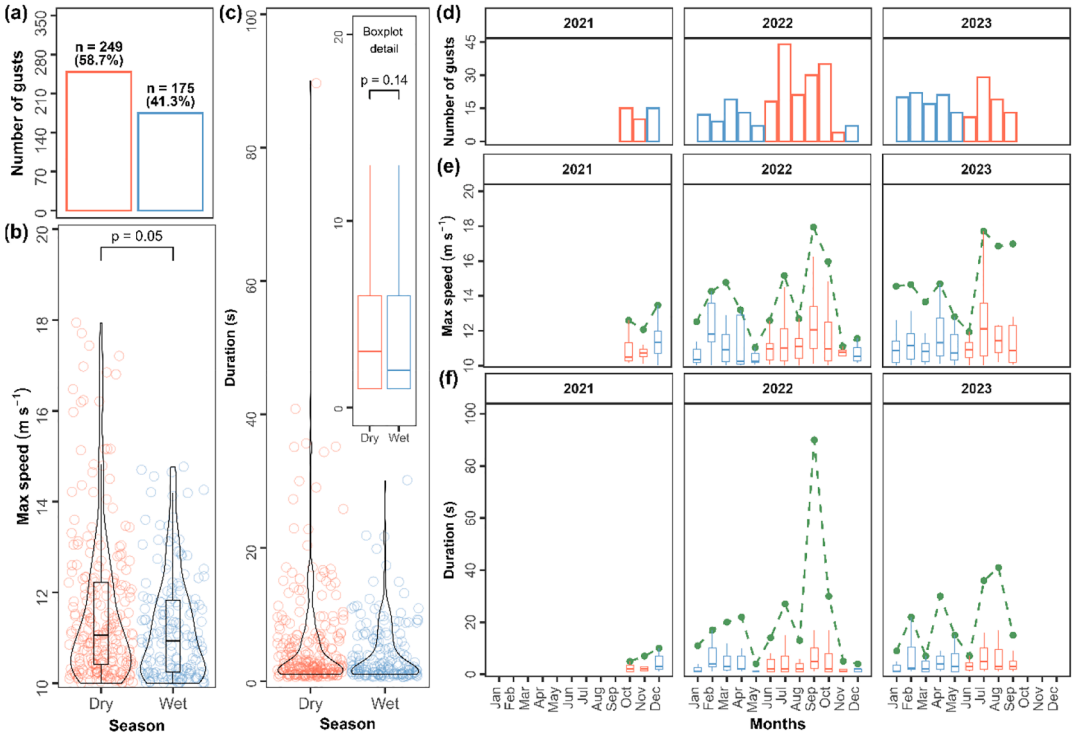


Fig. 5. Seasonal and monthly variation in strong canopy wind gust attributes. (a) Number of events by season; (b) maximum wind speed (m s^{-1}); (c) strong-gust duration (s); (d) monthly number of events; (e) monthly variation in maximum wind speed; and (f) monthly variation in strong-gust duration. In panels (d)–(f), months are classified according to dry and wet seasons. In panels (e) and (f), green points indicate monthly maximum values. All attributes were calculated using tower-specific detections without distinction among topographic positions.

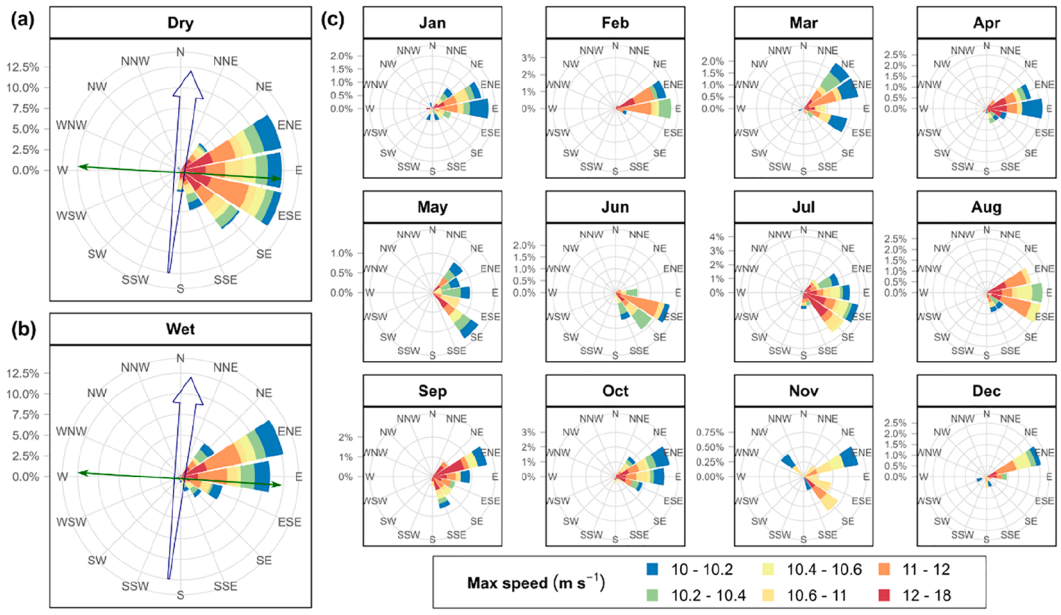


Fig. 6. Seasonal and monthly variation in wind direction of strong canopy wind gusts. (a) Wind direction distribution during the dry season; (b) wind direction distribution during the wet season; and (c) monthly variation in wind direction. The radial axis represents the frequency (%) of events by direction. All attributes were calculated using tower-specific detections without distinction among topographic positions. Green arrows indicate the alignment of the towers in panels (a) and (b), and blue arrows indicate the orientation of the valley in the vicinity of the towers, following the local topographic gradient from the headwater downslope.

rainfall explained 84% of the variation in the number of events and 68% of the variation in strong-gust duration (Fig. 7j and l). These relationships reflect patterns observed within the study period and were primarily associated with events occurring during the dry season. In contrast, no significant relationship was observed for maximum wind speed at 87th percentile ($R^2 = 0.67$, $p = 0.39$; Fig. 7k).

To provide additional context, rainfall patterns were also analyzed independently of wind gust attributes (Fig. S5). No clear relationship was found between wind gust attributes and monthly maximum rainfall rates (Fig. S5c–e). Median rainfall rates did not differ between dry and wet seasons (Fig. S5a), although a higher number of high-intensity rainfall events ($\geq$40 mm h^{-1}) was recorded during the wet season (approximately 30% more events), particularly in February and March (Fig. S5b).

3.4. Sensitivity to wind speed threshold

To evaluate the sensitivity of our results to the selected wind speed threshold ($\geq$10 m s^{-1}), we repeated the analyses across a range of thresholds from 10 to 17 m s^{-1}, corresponding to the range of wind speeds observed during the measurement period (see details in the Supplementary Material, Text S2; Fig. S6). Across all thresholds, consistent patterns were observed. Increasing the threshold resulted in a monotonic decrease in the number of detected events, accompanied by increases in both median maximum wind speed and strong-gust duration. These trends were consistent across topographic positions and between dry and wet seasons. Importantly, the relative differences among topographic positions were preserved across thresholds, with more exposed locations consistently experiencing higher wind speeds and longer gust durations. These results indicate that the main patterns reported in this study are robust and not dependent on the specific threshold used to define strong canopy wind gusts.

4. Discussion

4.1. Topographic and seasonal variation in strong canopy wind gusts

Wind gust attributes exhibited strongly asymmetric distributions, characterized by a predominance of low-intensity events and a smaller fraction of high-intensity events (Fig. S3). This pattern is consistent with previous descriptions of wind gust behavior (Monahan, 2006) and has been widely reported across tropical and temperate environments (Andreae et al., 2015; Bunkers and Hjelmfelt, 2021; Espinoza et al., 2012; Gardiner, 2021; Gomes and Vickery, 1978; McCay, 2003). It underscores the importance of upper-tail events in shaping canopy-level wind dynamics, even when median conditions remain relatively stable.

Differences across the topographic gradient were more pronounced in strong-gust duration and in the upper range of wind speeds than in median speeds. This indicates that spatial variability in the study area is primarily associated with the occurrence and persistence of higher-intensity events rather than systematic differences in background wind conditions. Similar patterns have been reported in other forests where topographic exposure and flow acceleration exert stronger control on extreme gusts than on mean wind conditions (Belcher et al., 2012; Mikita and Klimánek, 2012; Mitchell, 2013; Ruel et al., 2001; Tóta et al., 2012).

This modulation depends on the alignment between wind trajectories and local relief (Doane et al., 2023). In our study, the orientation of the plateau–slope–valley gradient is approximately perpendicular to the predominant gust direction (Fig. 4), which likely contributes to wind attenuation within the valley. The distinct wind direction patterns observed at the valley relative to the plateau and slope (Fig. 1c) further support the influence of local terrain configuration on airflow organization near the canopy (Belcher et al., 2012; Mendonça et al., 2025). In particular, the alignment between prevailing easterly winds (Rehbein et al., 2019, 2018) and local topography likely contributes to directional variability, consistent with studies of flow over complex forested terrain (Belcher et al., 2008; Finnigan, 2004; Quine et al., 2021). Channeling effects within the valley—previously described in adjacent forests with similar structure (Tóta et al., 2012)—may further modify wind direction and reduce horizontal wind speed, although this cannot be fully assessed using our two-dimensional anemometer data.

Temporal patterns in wind gust occurrence were consistent with the diurnal cycle of convection in the Central Amazon, with a higher frequency of events during daytime (Machado et al., 2004; Nunes et al., 2016; Rehbein et al., 2018; Rehbein and Ambrizzi, 2023). This pattern

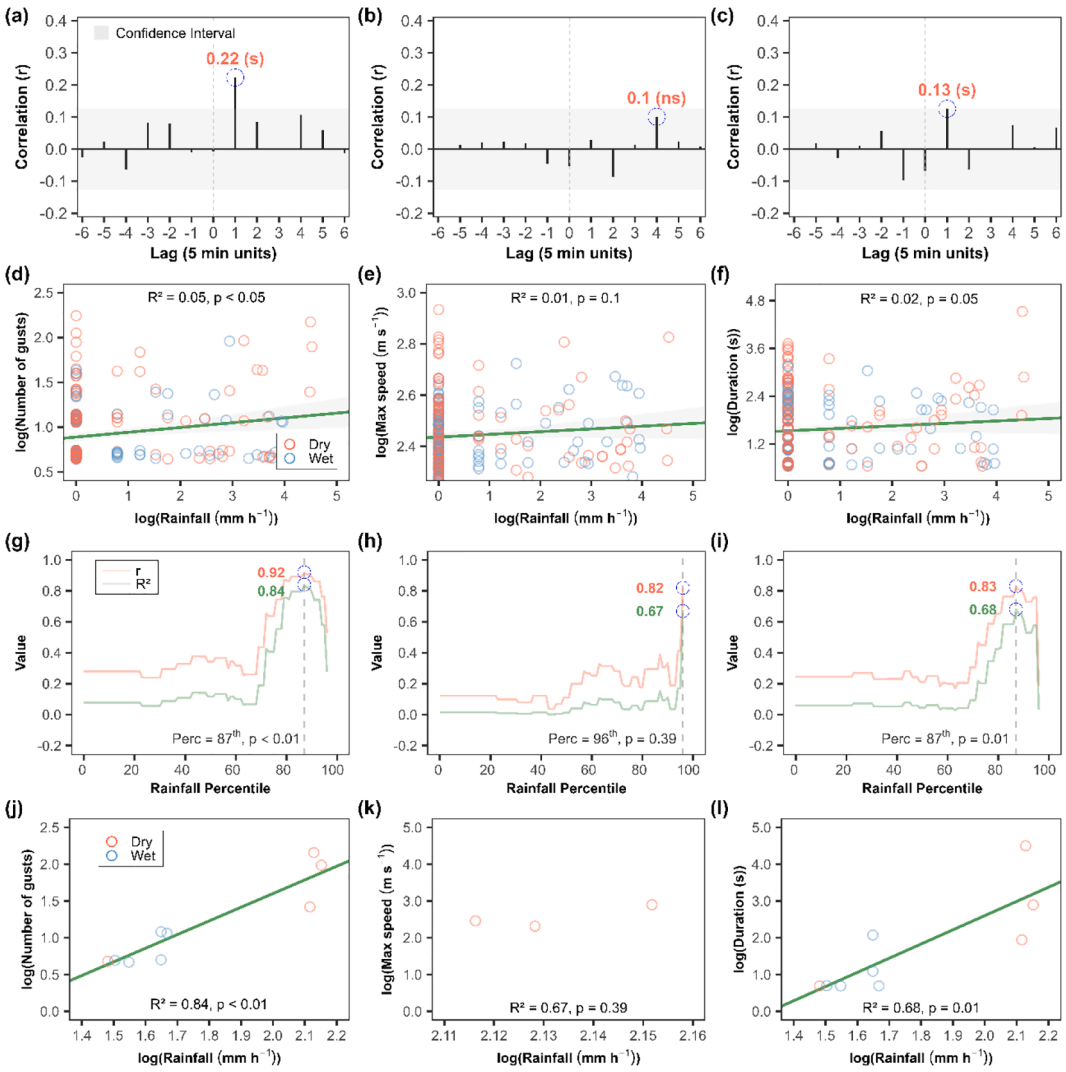


Fig. 7. Relationship between rainfall rate and strong canopy wind gust attributes. (a–c) Cross-correlation between log-transformed rainfall rate (mm h^{-1}) and log-transformed (a) number of events, (b) maximum wind speed, and (c) strong-gust duration. Pearson correlation coefficients (r) are shown, with significance levels indicated as "ns" (non-significant) and "s" (significant). (d–f) Linear relationships between log-transformed rainfall rate and log-transformed (d) number of events, (e) maximum wind speed, and (f) strong-gust duration. (g–i) Pearson correlation (r) and adjusted coefficient of determination (R^2) calculated across rainfall percentiles (0th–99th). Blue circles indicate the percentile at which the strongest statistical relationship was observed. (j–l). Linear relationships corresponding to the percentile with the strongest association between rainfall rate and strong canopy wind gust attributes. Grey bands in panels (a–f) represent confidence intervals (cross-correlation functions in a–c and regression fits in d–f). All attributes were calculated using tower-specific detections without distinguishing among topographic positions.

is associated with enhanced atmospheric instability, vertical mixing, and convective activity during daytime heating (Mendonça et al., 2023; Rehbein and Ambrizzi, 2023; Zhuang et al., 2017). However, the absence of significant differences in median wind speed and gust duration between daytime and nighttime suggests that the processes controlling event frequency differ from those governing event intensity.

During the two annual cycles monitored, the increased occurrence of strong canopy wind gusts during the dry season and their intensification during the transition to the wet season were consistent with previous observations suggesting more organized and vigorous convective systems during these periods in the Central Amazon (Ahlm et al., 2010; Andreae et al., 2015; Mendonça et al., 2023). Given this limited temporal coverage, these patterns should be regarded as observations from the study period rather than as a general seasonal behavior at the site. Nevertheless, the occurrence of strong gusts throughout the year indicates that multiple atmospheric processes contribute to their generation (Nobre et al., 2009). Overall, these results highlight that variability in strong canopy wind gusts reflects the combined influence of atmospheric processes operating across temporal scales and local terrain-related controls.

4.2. *Atmospheric conditions associated with potential forest disturbance*

The patterns of strong canopy wind gusts observed in this study provide insights into atmospheric conditions potentially associated with forest disturbance processes (Garstang et al., 1998; Mendonça et al., 2023; Oliveira et al., 2026), although no direct measurements of tree damage or mortality were systematically carried during the monitoring period. Previous studies have shown that strong winds alone are not sufficient to predict canopy damage, as disturbance outcomes depend on multiple interacting factors, including atmospheric conditions, site characteristics, and species-specific mechanical properties (Abd Latif and Blackburn, 2010; Gardiner, 2021; Lorenz et al., 2024).

In this context, the higher values of strong-gust duration and the occurrence of more intense events at exposed topographic positions and during seasonal transitions may indicate periods and locations where atmospheric conditions may favor canopy disturbance (Bunkers and Hjelmfelt, 2021). However, these patterns do not necessarily

correspond to the spatial distribution of observed forest disturbance. For example, studies in Amazon forests have reported higher windthrow-related mortality in valleys and during wetter periods, contrasting with the distribution of wind gust intensity observed here (Aleixo et al., 2019; Araujo et al., 2021; Esquivel-Muelbert et al., 2020; Fontes et al., 2018; Gora et al., 2025). This pattern, however, shall reflect differences in forest structure and diversity together with soil-root and crown-lianas interactions, which are still not fully addressed for tropical forests.

Independent observations at the INVENTA plot provide additional context on disturbance processes. Although a systematic inventory was not carried out during the study period, small-scale disturbances from falling branches and mortality of individual or small clusters of trees were observed. Similar disturbance patterns in the INVENTA plot were reported by Simonetti et al (2023), who identified several canopy gaps between 2018 and 2021 using RGB drone imagery. These authors also observed higher rates of disturbance during the transition from the dry to the wet season. Although these observations were collected in different periods, this seasonal pattern is consistent with the increased frequency and intensity of strong canopy wind gusts identified in our study.

In addition, a localized blowdown event affecting approximately four larger trees was recorded near the valley tower between October and November 2025. Although the exact timing of this event could not be determined, wind measurements from this period indicate peak wind speeds of approximately 25 m s^{-1}. Field observations indicated structural damage consistent with windthrow, including stem breakage near the base and uprooting of trees. Photographic and video evidences of this disturbance are provided in the Supplementary Material (Text S3; Fig. S7 – S11; Video S1).

While the absence of precise temporal correspondence prevents direct attribution of this event to specific wind gusts, this observation highlights that more severe disturbance events can also occur within the study area. Together, these observations suggest that disturbance regimes at the site likely span a continuum from frequent small-scale events to less frequent, higher-intensity disturbances, reinforcing the relevance of upper-tail wind gusts on shaping patterns of tree damage and mortality in Amazon forests.

Rainfall patterns further illustrate the complexity of these processes. Extreme rainfall events at INVENTA were 30% more frequent during the wet season (Fig. S5b), whereas stronger wind gusts were more common during the dry-to-wet transition (Fig. S5c-e). Cross-correlation analyses showed that associations between rainfall rate and wind gust attributes increased toward higher rainfall intensities, with the strongest relationships observed near the upper end of the distribution. These relationships should be interpreted as statistical associations rather than causal thresholds and reflect the heterogeneous nature of convective systems in the region (Nunes et al., 2016; Rehbein and Ambrizzi, 2023).

Conditions involving the co-occurrence of intense rainfall and strong winds have been associated with increased likelihood of forest disturbance in previous studies (Garstang et al., 1998; Negrón-Juárez et al., 2017, 2010; Nelson et al., 1994). However, disturbance outcomes depend on multiple interacting factors and cannot be inferred directly from atmospheric variables alone (Esquivel-Muelbert et al., 2020; Gora and Esquivel-Muelbert, 2021; McDowell et al., 2018; Negron-Juarez et al., 2023). More broadly, wind-related forest disturbance in the Amazon has been linked to a combination of atmospheric forcing and site-specific environmental conditions, with windstorms contributing substantially to observed tree damage and mortality in some regions reported in forest inventories (Aleixo et al., 2019; Esquivel-Muelbert et al., 2020; Fontes et al., 2018; Kattge et al., 2020). In this context, our results contribute to identifying atmospheric conditions that may be associated with increased windthrow frequency and severity (Urquiza-Muñoz et al., 2024), without directly quantifying ecological outcomes.

4.3. Study limitations and uncertainties

Wind measurements were obtained from three towers distributed along a single toposequence, which constrains the spatial representativeness of the results. Wind conditions in forested environments can vary substantially over short distances due to local topography, canopy structure, and atmospheric variability (Quine et al., 2021; Ruel et al., 2001). Furthermore, upscaling the observed gust patterns requires caution due to local factors such as valley orientation and altitude (Rennó et al., 2008; Tóta et al., 2012; Wang and Chen, 2025). Therefore, the patterns described here should be interpreted as representative of the monitored locations rather than of broader regional conditions.

Rainfall was measured at a single location, whereas storm systems in the Amazon exhibit strong spatial variability (Negrón-Juárez et al., 2017; Oliveira et al., 2026; Rehbein et al., 2019, 2018), and rainfall variability within the INVENTA tower network itself was not directly assessed. The assumption of limited local variability rests on the short distance between towers (~160 m), repeated field observations at the site, and indirect evidence from a nearby site (ATTO, see Section 2.2), rather than on direct measurements across the INVENTA network. As a result, the relationships observed between rainfall and wind gust attributes may reflect partial coupling between local rainfall measurements and wind conditions influenced by storms occurring outside the immediate vicinity of the towers. This limitation is particularly relevant given the non-stationary nature of convective processes in the region (Giangrande et al., 2023; Oliveira et al., 2026; Rehbein et al., 2019).

Our analysis covers a 24-month monitoring period that includes years influenced by large-scale climate anomalies (La Niña in 2022 and El Niño in 2023-2024, NOAA, 2024). These conditions are known to affect rainfall regimes and atmospheric dynamics in the Amazon (de Souza et al., 2021; Espinoza et al., 2019; Segura et al., 2020), and may have influenced the patterns we observed during the study period. Longer-term observations are needed to assess the persistence and variability of these patterns under different climatic conditions (Feng et al., 2023; Ferreira et al., 2026), and to expand the spatial coverage with additional sites (Andreae et al., 2015; Garstang et al., 1998; Martin et al., 2016).

Wind measurements were conducted at canopy height using two-dimensional sonic anemometers, which capture horizontal wind components but do not resolve vertical motions (Cuerva and Sanz-Andrés, 2000). Because vertical wind dynamics play an important role in convective systems and flow over complex terrain, their absence limits the interpretation of airflow processes (Belcher et al., 2008; Finnigan, 2000).

Additionally, rainfall measurements during strong wind gusts may be affected by wind-induced undercatch, since strong airflow can deflect precipitation particles away from the collector area, a limitation explicitly acknowledged in the instrument manufacturer guidelines. This may introduce further uncertainty in the observed rainfall–wind relationships.

Finally, the threshold used to define strong canopy wind gusts (10 m s^{-1}) represents an operational criterion based on the statistical distribution of wind speeds and supported by previous experimental estimates of tree mechanical stability in the same forest (see threshold of 10.75 m s^{-1} suggested by Peterson et al.(2019) based on empirical data from Ribeiro et al., 2016). However, given the wide variation in species composition and mechanical properties in Amazon trees, this threshold should not be interpreted as a universal indicator of tree damage. Establishing a direct link between these gusts and canopy damage would require concurrent measurements such as tree sway or strain monitoring, systematic post-storm damage surveys (e.g., repeated ground-based or drone-based canopy inventories), and species-specific mechanical property data, none of which were available in this study. Future studies integrating these elements — species-specific traits, tree-liana interactions, and direct disturbance measurements — are needed to better understand the relationship between wind conditions

and ecological outcomes (Magnabosco Marra et al., 2018; Phillips et al., 2005; Van Emmerik et al., 2018, 2017).

5. Conclusions

Strong canopy wind gusts occur throughout the year across the topographic gradient studied in a Central Amazon *terra-firme* forest. This consistent pattern reflects the interaction between atmospheric processes and local terrain configuration. Variability is expressed primarily through the intensity and duration of less frequent events rather than through background wind conditions. Elevated plateau areas more frequently experienced stronger and longer-lasting gusts, suggesting increased exposure to high-intensity atmospheric disturbances relative to lower topographic positions.

During the two years monitored, stronger and more persistent gusts were more frequently observed during the transition from the dry to the wet season, an observation consistent with periods of enhanced convective activity. Associations between rainfall intensity and wind gust characteristics increased toward the upper range of the rainfall distribution, although these relationships were not characterized by simultaneous co-occurrence. Instead, wind gusts frequently preceded rainfall by several minutes, a pattern consistent with convective outflow processes and indicative of spatial and temporal decoupling between wind and rainfall.

Our findings highlight the importance of high-frequency, in situ meteorological measurements for characterizing wind regimes in tropical forests, which are often not adequately resolved by remote sensing products and reanalysis datasets. By identifying atmospheric conditions associated with more intense wind activity, this study contributes to improving the characterization of wind dynamics in the Amazon. Although the broader applicability of our 10 m s^{-1} threshold should be evaluated cautiously across different Amazon forest types and environmental conditions, the approach presented here provides a practical basis for future monitoring efforts aimed at characterizing strong wind events and associated tree damage and mortality in tropical forests.

Data availability

The meteorological data used in this study are available upon request through the Amazon Tall Tower Observatory (ATTO) Data Portal (https://www.attodata.org, ID 691). Access may be granted following ATTO data policies and collaboration agreements.

Funding

This research is part of the Wind–Tree Interactions Project (INVENTA) and the Amazon Tall Tower Observatory (ATTO), funded by the German Federal Ministry of Research, Technology and Space – BMFTR (formerly BMBF; contract numbers 01LK2402E and 01LK2101A), the Brazilian Ministério da Ciência, Tecnologia e Inovação (MCTI/FINEP processes 01.11.0248.00, 01.22.0258.00, 01.22.0258.01), as well as by the Fundação de Amparo à Pesquisa do Estado do Amazonas (FAPEAM), and the Max Planck Society (MPG). INVENTA and this study were supported by the National Institute of Science and Technology – INCT Madeiras da Amazônia (Public Call MCTI/CNPq/CAPES/FAPEAM no. 16/2014), the Conselho Nacional de Desenvolvimento Científico e Tecnológico (CNPq), and the Coordenação de Aperfeiçoamento de Pessoal de Nível Superior (CAPES) – Finance Code 001. L.E. received funding from the Fundação de Amparo à Pesquisa do Estado do Amazonas (FAPEAM; PhD grant no. 41640. UNI739.1607.28032019-65939). R.I.N.-J. was funded by the U.S. Department of Energy's Office of Science, Office of Biological and Environmental Research, under Agreement Grant DE-AC02-05CH11231, through the Next Generation Ecosystem Experiments–Tropics and the Regional and Global Model Analysis Program's RUBISCO SFA (Reducing Uncertainties in Biogeochemical Interactions through Synthesis and Computation). C. Q. Dias-Júnior acknowledges support from CNPQ, Brazil (Processes 406884/2022-6, 307530/2022-1,406307/2023-7, 444929/2024-0, 445451/2024-6, 404254/2024-1).

Conflicts of Interest

The authors declare no conflicts of interest. The funders had no role in the design of the study; in the collection, analysis, or interpretation of data; in the writing of the manuscript, or in the decision to publish the results.

CRediT authorship contribution statement

Luciano Emmert: Writing – review & editing, Writing – original draft, Visualization, Validation, Methodology, Investigation, Formal analysis, Data curation, Conceptualization. **Susan Trumbore:** Writing – review & editing, Resources, Funding acquisition, Conceptualization. **Joaquim dos Santos:** Writing – review & editing, Project administration. **Adriana Simonetti:** Writing – review & editing. **Adriano José Nogueira Lima:** Writing – review & editing, Project administration. **Niro Higuchi:** Writing – review & editing. **Robinson Isaac Negrón-Juárez:** Writing – review & editing, Methodology. **Cléo Quaresma Dias-Júnior:** Writing – review & editing, Methodology. **Tarek El-Madany:** Writing – review & editing, Methodology. **Olaf Kolle:** Writing – review & editing, Methodology. **Gabriel Henrique Pires de Mello Ribeiro:** Writing – review & editing, Conceptualization. **Daniel Magnabosco Marra:** Writing – review & editing, Writing – original draft, Validation, Supervision, Resources, Project administration, Methodology, Investigation, Funding acquisition, Conceptualization.

Declaration of competing interest

The authors declare that they have no known competing financial interests or personal relationships that could have appeared to influence the work reported in this paper.

Acknowledgments

We are grateful for the logistical support provided by the field crew of the Forest Management Laboratory at the National Institute for Amazonian Research (INPA). We also thank Martin Hertel (*in memoriam*) from the Max Planck Institute for Biogeochemistry for his assistance during the instrumentation of the INVENTA towers.

Supplementary materials

Supplementary material associated with this article can be found, in the online version, at doi:10.1016/j.agrformet.2026.111504.

Data availability

Data will be made available on request.

References

Abd Latif, Z., Blackburn, G.A., 2010. The effects of gap size on some microclimate variables during late summer and autumn in a temperate broadleaved deciduous forest. Int. J. Biometeorol. 54, 119–129. https://doi.org/10.1007/s00484-009-0260-1.

Ahlm, L., Nilsson, E.D., Krejci, R., Mårtensson, E.M., Vogt, M., Artaxo, P., 2010. A comparison of dry and wet season aerosol number fluxes over the Amazon rain forest. Atmos. Chem. Phys. 10, 3063–3079. https://doi.org/10.5194/acp-10-3063-2010.

Albrecht, R.I., Morales, C.A., Silva Dias, M.A.F., 2011. Electrification of precipitating systems over the Amazon: physical processes of thunderstorm development. J. Geophys. Res. 116, D08209. https://doi.org/10.1029/2010JD014756.

Aleixo, I., Norris, D., Hemerik, L., Barbosa, A., Prata, E., Costa, F., Poorter, L., 2019. Amazonian rainforest tree mortality driven by climate and functional traits. Nat. Clim. Chang. 9, 384–388. https://doi.org/10.1038/s41558-019-0458-0.

Andreae, M.O., Acevedo, O.C., Araùjo, A., Artaxo, P., Barbosa, C.G.G., Barbosa, H.M.J., Brito, J., Carbone, S., Chi, X., Cintra, B.B.L., da Silva, N.F., Dias, N.L., Dias-Júnior, C. Q., Ditas, F., Ditz, R., Godoi, A.F.L., Godoi, R.H.M., Heimann, M., Hoffmann, T., Kesselmeier, J., Könemann, T., Krüger, M.L., Lavric, J.V., Manzi, A.O., Lopes, A.P., Martins, D.L., Mikhailov, E.F., Moran-Zuloaga, D., Nelson, B.W., Nölscher, A.C., Santos Nogueira, D., Piedade, M.T.F., Pöhlker, C., Pöschl, U., Quesada, C.A., Rizzo, L. V., Ro, C.-U., Ruckteschler, N., Sá, L.D.A., de Oliveira Sá, M., Sales, C.B., dos Santos, R.M.N., Saturno, J., Schöngart, J., Sörgel, M., de Souza, C.M., de Souza, R.A. F., Su, H., Targhetta, N., Tóta, J., Trebs, I., Trumbore, S., van Eijck, A., Walter, D., Wang, Z., Weber, B., Williams, J., Winderlich, J., Wittmann, F., Wolff, S., Yáñez-Serrano, A.M., 2015. The Amazon Tall Tower Observatory (ATTO): overview of pilot measurements on ecosystem ecology, meteorology, trace gases, and aerosols. Atmos. Chem. Phys. 15, 10723–10776. https://doi.org/10.5194/acp-15-10723-2015.

Araujo, R.F., Grubinger, S., Celes, C.H.S., Negrón-Juárez, R.I., Garcia, M., Dandois, J.P., Muller-Landau, H.C., 2021. Strong temporal variation in treefall and branchfall rates in a tropical forest is related to extreme rainfall: results from 5 years of monthly drone data for a 50 ha plot. Biogeosciences 18, 6517–6531. https://doi.org/10.5194/bg-18-6517-2021.

Araújo, R.F.d., 2019. Estrutura do dossel, dinâmica florestal e fenologia foliar com uso de aeronave remotamente pilotada na Amazônia (PhD thesis). Instituto Naciona de Pesquisas da Amazônia, INPA, Manaus, AM, Brasil.

Barry, R.G., Chorley, R.J., 2003. Atmosphere, weather and climate: eighth edition, atmosphere, weather and climate: eighth edition. https://doi.org/10.4324/9780203428238.

Belcher, S.E., Finnigan, J.J., Harman, I.N., 2008. Flows through forest canopies in complex terrain. Ecol. Appl. 18, 1436–1453. https://doi.org/10.1890/06-1894.1.

Belcher, S.E., Harman, I.N., Finnigan, J.J., 2012. The wind in the willows: flows in forest canopies in complex terrain. Annu. Rev. Fluid Mech. *44*, 479-504,. https://doi.org/10.1146/annurev-fluid-120710-101036.

Beljaars, A.C.M., 1987. The influence of sampling and filtering on measured wind gusts. J. Atmos. Ocean. Technol. 4, 613–626. https://doi.org/10.1175/1520-0426(1987)004<0613:TIOSAF>2.0.CO;2.

Bezerra, V.L., Dias-Júnior, C.Q., Vale, R.S., Santana, R.A., Botía, S., Manzi, A.O., Cohen, J.C.P., Martins, H.S., Chamecki, M., Fuentes, J.D., 2021. Near-surface atmospheric turbulence in the presence of a squall line above a forested and deforested region in the central amazon. Atmosphere 12, 461. https://doi.org/10.3390/atmos12040461.

Braga, P.I.S., 1979. Subdivisão fitogeográfica, tipos de vegetação, conservação e inventário florístico da floresta amazônica. Acta Amaz. *9*, 53-80,. https://doi.org/10.1590/1809-43921979094s053.

Brando, P.M., Barlow, J., Macedo, M.N., Silvério, D.V., Ferreira, J.N., Maracahipes, L., Anderson, L., Morton, D.C., Alencar, A., Paolucci, L.N., Jacobs, S., Stouter, H., Randerson, J., Flores, B.M., Starinchak, B., Coe, M., Pires, M.M., Rattis, L., Armenteras, D., Artaxo, P., Ordway, E.M., Trumbore, S., Staver, C., Berenguer, E., Menor, I.O., Maracahipes-Santos, L., Potter, N., Spracklen, D.V., Uribe, M., 2025. Tipping points of Amazonian forests: beyond myths and toward solutions. Annu. Rev. Environ. Resour. 50, 97–131. https://doi.org/10.1146/annurev-environ-111522-112804.

Bunkers, M.J., Hjelmfelt, M.R., 2021. Thunderstorm downbursts: windstorms and blowdowns. In: Johnson, A.E., Miyanishi, K. (Eds.), Plant Disturbance Ecology. Elsevier, Burlington, MA, pp. 65–115. https://doi.org/10.1016/B978-0-12-818813-2.00003-4.

Carneiro, V.M.C., 2004. Composição florística e análise estrutural da floresta primária de terra firme na bacia do rio cuieiras, Manaus-Am (Master Dissertation). Universidade Federal do Amazônas, Manaus, AM, Brazil.

Chambers, J.Q., Negron-Juarez, R.I., Marra, D.M., Di Vittorio, A., Tews, J., Roberts, D., Ribeiro, G.H.P.M., Trumbore, S.E., Higuchi, N., 2013. The steady-state mosaic of disturbance and succession across an old-growth Central Amazon forest landscape. In: Proceedings of the National Academy of Sciences. https://doi.org/10.1073/pnas.1202894110.

Chauvel, A., Lucas, Y., Boulet, R., 1987. On the genesis of the soil mantle of the region of Manaus, Central Amazonia, Brazil. Experientia 43, 234–241. https://doi.org/10.1007/BF01945546/METRICS.

Cuerva, A., Sanz-Andrés, A., 2000. On sonic anemometer measurement theory. J. Wind Eng. Ind. Aerodyn. 88, 25–55. https://doi.org/10.1016/S0167-6105(00)00023-4.

Cunha, H.F.V., Andersen, K.M., Lugli, L.F., Santana, F.D., Aleixo, I.F., Moraes, A.M., Garcia, S., Di Ponzio, R., Mendoza, E.O., Brum, B., Rosa, J.S., Cordeiro, A.L., Portela, B.T.T., Ribeiro, G., Coelho, S.D., de Souza, S.T., Silva, L.S., Antonieto, F., Pires, M., Salomão, A.C., Miron, A.C., de Assis, R.L., Domingues, T.F., Aragão, L.E.O. C., Meir, P., Camargo, J.L., Manzi, A.O., Nagy, L., Mercado, L.M., Hartley, I.P., Quesada, C.A., 2022. Direct evidence for phosphorus limitation on Amazon forest productivity. Nature 608, 558–562. https://doi.org/10.1038/s41586-022-05085-2.

Dag, O., Dolgun, A., Konar, Naime, M., 2018. onewaytests: an R package for one-way tests in independent groups designs. R J. 10, 175. https://doi.org/10.32614/RJ-2018-022.

Davidson, M.R., Millstein, D., 2022. Limitations of reanalysis data for wind power applications. Wind Energy 25, 1646–1653. https://doi.org/10.1002/we.2759.

De Oliveira, A.A., Mori, S.A., Alexandre, O., Scott, M., De Oliveira, A.A., Mori, S.A., 1999. A central Amazonian terra firme forest. I. High tree species richness on poor soils. Biodivers. Conserv. *8*, 1219-1244,. https://doi.org/10.1023/A:1008908615271.

de Oliveira Santos, M., Stosic, T., Stosic, B.D., 2012. Long-term correlations in hourly wind speed records in Pernambuco, Brazil. Phys. A Stat. Mech. Appl. 391, 1546–1552. https://doi.org/10.1016/j.physa.2011.08.041.

De Santana, R.A.S., Dias-Júnior, C.Q., Do Vale, R.S., Tóta, J., Fitzjarrald, D.R., 2017. Observing and modeling the vertical wind profile at multiple sites in and above the amazon rain forest canopy. Adv. Meteorol. *2017*, 1-8,. https://doi.org/10.1155/2017/5436157.

de Souza, I.P., Andreoli, R.V., Kayano, M.T., Vargas, F.F., Cerón, W.L., Martins, J.A., Freitas, E., de Souza, R.A.F., 2021. Seasonal precipitation variability modes over South America associated to El Niño-Southern Oscillation (<scp>ENSO</scp>and <scp>non-ENSO</scp>components during the 1951–2016 period. Int. J. Climatol. 41, 4321–4338. https://doi.org/10.1002/joc.7075.

Doane, T.H., Yanites, B.J., Edmonds, D.A., Novick, K.A., 2023. Hillslope roughness reveals forest sensitivity to extreme winds. In: Proceedings of the National Academy of Sciences, 120, e2212105120. https://doi.org/10.1073/pnas.2212105120.

dos Anjos, P.S., da Silva, A.S.A., Stošić, B., Stošić, T., 2015. Long-term correlations and cross-correlations in wind speed and solar radiation temporal series from Fernando de Noronha Island, Brazil. Phys. A Stat. Mech. Appl. 424, 90–96. https://doi.org/10.1016/j.physa.2015.01.003.

Dunlop, S., 2017. Weather: A Very Short Introduction, 2nd ed, Find Print Edition in Library Weather: A Very Short Introduction. Oxford University Press (OUP), United Kingdom. https://doi.org/10.1093/actrade/9780199571314.001.0001.

Emmert, L., Negrón-Juárez, R.I., Chambers, J.Q., dos Santos, J., Lima, A.J.N., Trumbore, S., Marra, D.M., 2023. Sensitivity of optical satellites to estimate windthrow tree-mortality in a central amazon forest. Remote Sens. 15, 4027. https://doi.org/10.3390/rs15164027.

England, A.H., 2000. A dynamic analysis of windthrow of trees. Forestry 73, 225–238. https://doi.org/10.1093/forestry/73.3.225.

Espinoza, J.C., Lengaigne, M., Ronchail, J., Janicot, S., 2012. Large-scale circulation patterns and related rainfall in the Amazon Basin: a neuronal networks approach. Clim. Dyn. *38*, 121-140,. https://doi.org/10.1007/s00382-011-1010-8.

Espinoza, J.C., Ronchail, J., Marengo, J.A., Segura, H., 2019. Contrasting North–South changes in Amazon wet-day and dry-day frequency and related atmospheric features (1981–2017). Clim. Dyn. 52, 5413–5430. https://doi.org/10.1007/s00382-018-4462-2.

Esquivel-Muelbert, A., Phillips, O.L., Brienen, R.J.W., Fauset, S., Sullivan, M.J.P., Baker, T.R., Chao, K.J., Feldpausch, T.R., Gloor, E., Higuchi, N., Houwing-Duistermaat, J., Lloyd, J., Liu, H., Malhi, Y., Marimon, B., Marimon Junior, B.H., Monteagudo-Mendoza, A., Poorter, L., Silveira, M., Torre, E.V., Dávila, E.A., del Aguila Pasquel, J., Almeida, E., Loayza, P.A., Andrade, A., Aragão, L.E.O.C., Araujo-Murakami, A., Arets, E., Arroyo, L., Aymard C, G.A., Baisie, M., Baraloto, C., Camargo, P.B., Barroso, J., Blanc, L., Bonal, D., Bongers, F., Boot, R., Brown, F., Burban, B., Camargo, J.L., Castro, W., Moscoso, V.C., Chave, J., Comiskey, J., Valverde, F.C., da Costa, A.L., Cardozo, N.D., 2020. Tree mode of death and mortality risk factors across Amazon forests. Nat. Commun. 11, 1–11. https://doi.org/10.1038/s41467-020-18996-3.

Faybishenko, B., Versteeg, R., Pastorello, G., Dwivedi, D., Varadharajan, C., Agarwal, D., 2022. Challenging problems of quality assurance and quality control (QA/QC) of meteorological time series data. Stoch. Environ. Res. Risk Assess. 36, 1049–1062. https://doi.org/10.1007/s00477-021-02106-w.

Feng, Y., Negrón-Juárez, R.I., Romps, D.M., Chambers, J.Q., 2023. Amazon windthrow disturbances are likely to increase with storm frequency under global warming. Nat. Commun. 14, 101. https://doi.org/10.1038/s41467-022-35570-1.

Ferraz, J., Ohta, S., de Sales, P.C., 1998. Distribuição dos solos ao longo de dois transectos em floresta primária ao Norte de Manaus (AM). MCT-INPA/JICA (Ed.), Pesquisas Florestais Para a Conservação Da Floresta e Reabilitação de Áreas Degradadas Da Amazônia. INPA, Manaus, AM, pp. 109–143.

Ferreira, V., Oliveira dos Santos, L., Ilha de Oliveira, M., de Lima Nascimento, E., Rammig, A., 2026. Climatology and Environmental Controls of Intense Wind Gusts in the Brazilian Amazon. Geophys. Res. Lett. 53, e2025GL120537. https://doi.org/10.1029/2025GL120537.

Filho, A.J.P., Carbone, R.E., Tuttle, J.D., Karam, H.A., 2015. Convective Rainfall in Amazonia and Adjacent Tropics. Atmos. Clim. Sci. 05, 137–161. https://doi.org/10.4236/acs.2015.52011.

Finnigan, J., 2000. Turbulence in Plant Canopies. Annu. Rev. Fluid Mech. 32, 519–571. https://doi.org/10.1146/annurev.fluid.32.1.519.

Finnigan, J., 2004. The footprint concept in complex terrain. Agric. For. Meteorol. 127, 117–129. https://doi.org/10.1016/J.AGRFORMET.2004.07.008.

Flores, B.M., Montoya, E., Sakschewski, B., Nascimento, N., Staal, A., Betts, R.A., Levis, C., Lapola, D.M., Esquível-Muelbert, A., Jakovac, C., Nobre, C.A., Oliveira, R. S., Borma, L.S., Nian, D., Boers, N., Hecht, S.B., ter Steege, H., Arieira, J., Lucas, I.L., Berenguer, E., Marengo, J.A., Gatti, L.V., Mattos, C.R.C., Hirota, M., 2024. Critical transitions in the Amazon forest system. Nat 626, 555–564. https://doi.org/10.1038/s41586-023-06970-0, 2024 6267999.

Fontes, C.G., Chambers, J.Q., Higuchi, N., 2018. Revealing the causes and temporal distribution of tree mortality in Central Amazonia. For. Ecol. Manage. *424*, 177-183,. https://doi.org/10.1016/j.foreco.2018.05.002.

Freire, L.S., Gerken, T., Ruiz-Plancarte, J., Wei, D., Fuentes, J.D., Katul, G.G., Dias, N.L., Acevedo, O.C., Chamecki, M., 2017. Turbulent mixing and removal of ozone within an Amazon rainforest canopy. J. Geophys. Res. Atmos. 122, 2791–2811. https://doi.org/10.1002/2016JD026009.

Fujita, T.T., 1981. Tornadoes and downbursts in the context of generalized planetary scales. J. Atmos. Sci. https://doi.org/10.1175/1520-0469(1981)038<1511:TADITC>2.0.CO;2.

Fujita, T.T., 1985. The downburst : microburst and macroburst : report of projects NIMROD and JAWS /T. Theodore Fujita. [Chicago] Satell. Mesometeorology Res. Proj. Dept. Geophys. Sci. Univ. Chicago SMRP resea 122.

Fujita, T.T., Wakimoto, R.M., 1983. MICROBURSTS IN JAWS DEPICTED BY DOPPLER RADARS. PAM, AND AERIAL PHOTOGRAPHS. Conference on Radar Meteorology of the American Meteorological Society.

Gandrud, C., 2016. DataCombine: Tools for Easily Combining and Cleaning Data Sets.

Gardiner, B., 2021. Wind damage to forests and trees: a review with an emphasis on planted and managed forests. J. For. Res. 26, 248–266. https://doi.org/10.1080/13416979.2021.1940665.
Gardiner, B., Achim, A., Nicoll, B., Ruel, J.-C., 2019. Understanding the interactions between wind and trees: an introduction to the IUFRO 8th Wind and Trees Conference (2017). For. An Int. J. For. Res. 92, 375–380. https://doi.org/10.1093/forestry/cpz044.
Garstang, M., Massie, H.L., Halverson, J., Greco, S., Scala, J., 1994. Amazon Coastal Squall Lines. Part I: Structure and Kinematics. Mon. Weather Rev. 122, 608–622. https://doi.org/10.1175/1520-0493(1994)122<0608:ACSLPI>2.0.CO;2.
Garstang, M., White, S., Shugart, H.H., Halverson, J., 1998. Convective cloud downdrafts as the cause of large blowdowns in the Amazon rainforest. Meteorol. Atmos. Phys. 67, 199–212. https://doi.org/10.1007/BF01277510.
Geitmann, A., Gril, J., 2018. Plant Biomechanics, Plant Biomechanics: From Structure to Function at Multiple Scales. Springer International Publishing, Cham. https://doi.org/10.1007/978-3-319-79099-2.
Giangrande, S.E., Biscaro, T.S., Peters, J.M., 2023. Seasonal controls on isolated convective storm drafts, precipitation intensity, and life cycle as observed during GoAmazon2014/5. Atmos. Chem. Phys. 23, 5297–5316. https://doi.org/10.5194/acp-23-5297-2023.
Gomes, L., Vickery, B.J., 1978. Extreme wind speeds in mixed wind climates. J. Wind Eng. Ind. Aerodyn. 2, 331–344. https://doi.org/10.1016/0167-6105(78)90018-1.
Gonçalves, M.B., Dias-Júnior, C.Q., D'Oliveira, F.A.F., Cely-Toro, I.M., Cohen, J.C.P., Martins, H.S., da Silva, G.H.S., de Araújo, A.C., Mortarini, L., 2024. Squall lines and turbulent exchange at the Amazon forest-atmosphere interface. Meteorol. Atmos. Phys. 136, 41. https://doi.org/10.1007/s00703-024-01039-7.
Gora, E.M., Esquivel-Muelbert, A., 2021. Implications of size-dependent tree mortality for tropical forest carbon dynamics. Nat. Plants 7, 384–391. https://doi.org/10.1038/s41477-021-00879-0.
Gora, E.M., McGregor, I.R., Muller-Landau, H.C., Burchfield, J.C., Cushman, K.C., Rubio, V.E., Mori, G.B., Sullivan, M.J.P., Chmielewski, M.W., Esquivel-Muelbert, A., 2025. Storms Are an Important Driver of Change in Tropical Forests. Ecol. Lett. 28, e70157. https://doi.org/10.1111/ele.70157.
Gotelli, N.J., Ellisson, A.M., 2013. A Primer of Ecological Statistics, 2nd ed. Associates, Sinauer, Sunderland, Massachusetts.
Greco, S., Scala, J., Halverson, J., Massie, H.L., Tao, W.-K., Garstang, M., 1994. Amazon Coastal Squall Lines. Part II: Heat and Moisture Transports. Mon. Weather Rev. 122, 623–635. https://doi.org/10.1175/1520-0493(1994)122<0623:ACSLPI>2.0.CO;2.
Harper, B.A., Kepert, J.D., Ginger, J.D., 2010. Guidelines for converting between various wind averaging periods in tropical cyclone conditions. Geneva, Switzerlan.
Harris, I., Osborn, T.J., Jones, P., Lister, D., 2020. Version 4 of the CRU TS monthly high-resolution gridded multivariate climate dataset. Sci. Data 7, 109. https://doi.org/10.1038/s41597-020-0453-3.
Hersbach, H., Bell, B., Berrisford, P., Hirahara, S., Horányi, A., Muñoz-Sabater, J., Nicolas, J., Peubey, C., Radu, R., Schepers, D., Simmons, A., Soci, C., Abdalla, S., Abellan, X., Balsamo, G., Bechtold, P., Biavati, G., Bidlot, J., Bonavita, M., De Chiara, G., Dahlgren, P., Dee, D., Diamantakis, M., Dragani, R., Flemming, J., Forbes, R., Fuentes, M., Geer, A., Haimberger, L., Healy, S., Hogan, R.J., Hólm, E., Janisková, M., Keeley, S., Laloyaux, P., Lopez, P., Lupu, C., Radnoti, G., de Rosnay, P., Rozum, I., Vamborg, F., Villaume, S., Thépaut, J., 2020. The ERA5 global reanalysis. Q. J. R. Meteorol. Soc. 146, 1999–2049. https://doi.org/10.1002/qj.3803.
Herve, M., 2023. RVAideMemoire: Testing and Plotting Procedures for Biostatistics.
Holmes, J.D., Allsop, A.C., Ginger, J.D., 2014. Gust durations, gust factors and gust response factors in wind codes and standards. Wind Struct 19, 339–352. https://doi.org/10.12989/was.2014.19.3.339.
Huffman, G.J., Bolvin, D.T., Braithwaite, D., Hsu, K., Joyce, R., Xie, P., Yoo, S.-H., 2020. NASA global precipitation measurement (GPM) integrated multi-satellite retrievals for GPM (IMERG) (No. Greenbelt, MD 20771). Algorithm Theoretical Basis Document (ATBD) Version, p. 6.
Hyndman, R., Athanasopoulos, G., Bergmeir, C., Caceres, G., Chhay, L., O'Hara-Wild, M., Petropoulos, F., Razbash, S., Wang, E., Yasmeen, F., 2024. forecast: Forecasting functions for time series and linear models.
Jackson, T., Shenkin, A., Kalyan, B., Zionts, J., Calders, K., Origo, N., Disney, M., Burt, A., Raumonen, P., Malhi, Y., 2019. A New Architectural Perspective on Wind Damage in a Natural Forest. Front. For. Glob. Chang. 1. *1*,. https://doi.org/10.3389/ffgc.2018.00013.
Kantz, H., Holstein, D., Ragwitz, M., Vitanov, N.K., 2004. Extreme events in surface wind: Predicting turbulent gusts. In: AIP Conference Proceedings. AIP, pp. 315–324. https://doi.org/10.1063/1.1846492.
Kassambara, A., 2023. rstatix: Pipe-Friendly Framework for Basic Statistical Tests.
Kattge, J., Bönisch, G., Díaz, S., 2020. TRY plant trait database – enhanced coverage and open access. Glob. Chang. Biol. *26*, 119-188,. https://doi.org/10.1111/gcb.14904.
Kavasseri, R.G., Nagarajan, R., 2004. Evidence of Crossover Phenomena in Wind-Speed Data. IEEE Trans. Circuits Syst. I Regul. Pap. 51, 2255–2262. https://doi.org/10.1109/TCSI.2004.836846.
Koçak, K., 2009. Examination of persistence properties of wind speed records using detrended fluctuation analysis. Energy 34, 1980–1985. https://doi.org/10.1016/j.energy.2009.08.006.
Kristensen, L., Casanova, M., Courtney, M.S., Troen, I., 1991. In search of a gust definition. Boundary-Layer Meteorol 55, 91–107. https://doi.org/10.1007/BF00119328.
Kristoufek, L., 2014. Measuring correlations between non-stationary series with DCCA coefficient. Phys. A Stat. Mech. its Appl. 402, 291–298. https://doi.org/10.1016/j.physa.2014.01.058.
Lima, A.J.N., 2010. Avaliacão de um sistema de inventário florestal contínuo em áreas manejadas e não manejadas do estado do Amazonas (AM). Ph.D. Diss. Univ. Fed. do Amaz. Manaus, Brazil 183 (in Port. with English Abstr. 183.
Lorenz, Rike, Becker, Nico, Gardiner, Barry, Ulbrich, Uwe, Hanewinkel, Marc, Schmitz, Benjamin, 2024. Storm damage beyond wind speed - Impacts of wind characteristics and other meteorological factors on tree fall along railway lines. Egusph 1–34. https://doi.org/10.5194/EGUSPHERE-2024-120 [preprint].
Luizão, F.J., Schubart, H.O.R., 1987. Litter production and decomposition in a terra-firme forest of Central Amazonia. Experientia *43*, 259-265,. https://doi.org/10.1007/BF01945549.
Machado, L.A.T., Laurent, H., Dessay, N., Miranda, I., 2004. Seasonal and diurnal variability of convection over the Amazonia: A comparison of different vegetation types and large scale forcing. Theor. Appl. Climatol. 78, 61–77. https://doi.org/10.1007/s00704-004-0044-9.
Magnabosco Marra, D., Trumbore, S.E., Higuchi, N., Ribeiro, G.H.P.M.P.M., Negrón-Juárez, R.I., Holzwarth, F., Rifai, S.W., dos Santos, J., Lima, A.J.N.N., Kinupp, V.F., Chambers, J.Q., Wirth, C., 2018. Windthrows control biomass patterns and functional composition of Amazon forests. Glob. Chang. Biol. 24, 5867–5881. https://doi.org/10.1111/gcb.14457.
Marengo, J.A., Liebmann, B., Kousky, V.E., Filizola, N.P., Wainer, I.C., 2001. Onset and End of the Rainy Season in the Brazilian Amazon Basin. J. Clim. 14, 833–852. https://doi.org/10.1175/1520-0442(2001)014<0833:OAEOTR>2.0.CO;2.
Marra, D.M., Chambers, J.Q., Higuchi, N., Trumbore, S.E., Ribeiro, G.H.P.M., Dos Santos, J., Negrón-Juárez, R.I., Reu, B., Wirth, C., 2014. Large-scale wind disturbances promote tree diversity in a Central Amazon forest. PLoS One *9*, e103711,. https://doi.org/10.1371/journal.pone.0103711.
Marra, D.M., Negrón-Juárez, R.I., Lima, A.J.N., Higuchi, N., Celes, C.H.S., Peterson, C.J., Chambers, J.Q., Kolle, O., Richter, R., Wirth, C., Trumbore, S., 2018. Wind-tree interactions in the Amazon (INVENTA): disturbance dynamics and forest functioning. AGU, Adv. Earth Sp. Scince - Fall Meet. 2018AGUFM.B51C04M.
Martin, S.T., Artaxo, P., Machado, L.A.T., Manzi, A.O., Souza, R.A.F., Schumacher, C., Wang, J., Andreae, M.O., Barbosa, H.M.J., Fan, J., Fisch, G., Goldstein, A.H., Guenther, A., Jimenez, J.L., Pöschl, U., Silva Dias, M.A., Smith, J.N., Wendisch, M., 2016. Introduction: Observations and Modeling of the Green Ocean Amazon (GoAmazon2014/5). Atmos. Chem. Phys 16, 4785–4797. https://doi.org/10.5194/acp-16-4785-2016.
Mauder, M., Cuntz, M., Drüe, C., Graf, A., Rebmann, C., Schmid, H.P., Schmidt, M., Steinbrecher, R., 2013. A strategy for quality and uncertainty assessment of long-term eddy-covariance measurements. Agric. For. Meteorol. 169, 122–135. https://doi.org/10.1016/j.agrformet.2012.09.006.
McCay, M.G., 2003. Winds under the Rain Forest Canopy: The Aerodynamic Environment of Gliding Tree Frogs. Biotropica 35, 94–102. https://doi.org/10.1111/J.1744-7429.2003.TB00266.X.
McDowell, N., Allen, C.D., Anderson-Teixeira, K., Brando, P., Brienen, R., Chambers, J., Christoffersen, B., Davies, S., Doughty, C., Duque, A., Espirito-Santo, F., Fisher, R., Fontes, C.G., Galbraith, D., Goodsman, D., Grossiord, C., Hartmann, H., Holm, J., Johnson, D.J., Kassim, A.R., Keller, M., Koven, C., Kueppers, L., Kumagai, T., Malhi, Y., McMahon, S.M., Mencuccini, M., Meir, P., Moorcroft, P., Muller-Landau, H.C., Phillips, O.L., Powell, T., Sierra, C.A., Sperry, J., Warren, J., Xu, C., Xu, X., 2018. Drivers and mechanisms of tree mortality in moist tropical forests. New Phytol *219*, 851-869,. https://doi.org/10.1111/nph.15027.
Mendonça, A.C.S., Dias-Júnior, C.Q., Acevedo, O.C., Marra, D.M., Cely-Toro, I.M., Fisch, G., Brondani, D.V., Manzi, A.O., Portela, B.T.T., Quesada, C.A., Mortarini, L., 2025. Estimation of the nocturnal boundary layer height over the Central Amazon forest using turbulence measurements. Agric. For. Meteorol. 367, 110469. https://doi.org/10.1016/j.agrformet.2025.110469.
Mendonça, A.C.S., Dias-Júnior, C.Q., Acevedo, O.C., Santana, R.A., Costa, F.D., Negrón-Juarez, R.I., Manzi, A.O., Trumbore, S.E., Marra, D.M., 2023. Turbulence regimes in the nocturnal roughness sublayer: Interaction with deep convection and tree mortality in the Amazon. Agric. For. Meteorol. 339, 109526. https://doi.org/10.1016/j.agrformet.2023.109526.
Mikita, T., Klimánek, M., 2012. Topographic Exposure and its Practical Applications. J. Landsc. Ecol. *3*, 42-51,. https://doi.org/10.2478/v10285-012-0022-3.
Minola, L., Zhang, F., Azorin-Molina, C., Pirooz, A.A.S., Flay, R.G.J., Hersbach, H., Chen, D., 2020. Near-surface mean and gust wind speeds in ERA5 across Sweden: towards an improved gust parametrization. Clim. Dyn. 55, 887–907. https://doi.org/10.1007/s00382-020-05302-6.
Mitchell, S.J., 2013. Wind as a natural disturbance agent in forests: A synthesis. Forestry *86*, 147-157,. https://doi.org/10.1093/forestry/cps058.
Mitsuta, Y., Tsukamoto, O., 1989. Studies on Spatial Structure of Wind Gust. J. Appl. Meteorol. 28, 1155–1160. https://doi.org/10.1175/1520-0450(1989)028<1155:SOSSOW>2.0.CO;2.
Moller, A.R., 2001. Severe Local Storms Forecasting, in: Severe Convective Storms. American Meteorological Society, Boston, MA, pp. 433–480. https://doi.org/10.1007/978-1-935704-06-5_11.
Monahan, A.H., 2006. The Probability Distribution of Sea Surface Wind Speeds. Part I: Theory and SeaWinds Observations. J. Clim. 19, 497–520. https://doi.org/10.1175/JCLI3640.1.
Moore, J.R., Maguire, D.A., 2004. Natural sway frequencies and damping ratios of trees: Concepts, review and synthesis of previous studies. Trees - Struct. Funct. *18*, 195-203,. https://doi.org/10.1007/s00468-003-0295-6.
Negrón-Juárez, R., Jenkins, H., Raupp, C., Riley, W., Kueppers, L., Magnabosco Marra, D., Ribeiro, G., Monteiro, M., Candido, L., Chambers, J., Higuchi, N., 2017. Windthrow Variability in Central Amazonia. Atmosphere (Basel) 8, 28. https://doi.org/10.3390/atmos8020028.

Negron-Juarez, R., Magnabosco-Marra, D., Feng, Y., Urquiza-Muñoz, J.D., Riley, W.J., Chambers, J.Q., 2023. Windthrow characteristics and their regional association with rainfall, soil, and surface elevation in the Amazon. Environ. Res. Lett. 18, 014030. https://doi.org/10.1088/1748-9326/acaf10.

Negrón-Juárez, R.I., Chambers, J.Q., Guimaraes, G., Zeng, H., Raupp, C.F.M., Marra, D. M., Ribeiro, G.H.P.M., Saatchi, S.S., Nelson, B.W., Higuchi, N., 2010. Widespread Amazon forest tree mortality from a single cross-basin squall line event. Geophys. Res. Lett. *37*,. https://doi.org/10.1029/2010GL043733.

Negrón-Juárez, R.I., Holm, J.A., Marra, D.M., Rifai, S.W., Riley, W.J., Chambers, J.Q., Koven, C.D., Knox, R.G., McGroddy, M.E., Di Vittorio, A.V., Urquiza-Muñoz, J., Tello-Espinoza, R., Muñoz, W.A., Ribeiro, G.H.P.M., Higuchi, N., 2018. Vulnerability of Amazon forests to storm-driven tree mortality. Environ. Res. Lett. *13*, 054021,. https://doi.org/10.1088/1748-9326/aabe9f.

Nelson, B.W., Kapos, V., Adams, J.B., Oliveira, W.J., Braun, O.P.G.G., 1994. Forest Disturbance by Large Blowdowns in the Brazilian Amazon. Ecology 75, 853–858. https://doi.org/10.2307/1941742.

NOAA (National Oceanic and Atmospheric Administration), 2024. ENSO Index [WWW Document]. Natl. Weather Serv. Clim. Predict. Cent. URL https://origin.cpc.ncep.noaa.gov/products/analysis_monitoring/ensostuff/ONI_v5.php accessed 5.17.24.

Nobre, C.A., Marengo, J.A., Artaxo, P., 2009. Understanding the climate of Amazonia: Progress from LBA. Amazonia and Global Change 145–147. https://doi.org/10.1029/2009GM000903.

Nunes, A.M.P.P., Silva Dias, M.A.F.F., Anselmo, E.M., Morales, C.A., 2016. Severe Convection Features in the Amazon Basin: A TRMM-Based 15-Year Evaluation. Front. Earth Sci. 4, 37. https://doi.org/10.3389/feart.2016.00037.

Ogle, D.H., Doll, J.C., Wheeler, A.P., Dinno, A., 2023. FSA: Simple Fisheries Stock Assessment Methods.

Oliveira, M.I., Mortarini, L., Acevedo, O.C., Cely-Toro, I.M., Grosso, M., Reis, L.I., Dias-Júnior, C.Q., Quesada, C.A., Ribeiro, B.Z., Brondani, D.V., 2026. Convective cold pools and attendant turbulence at the Amazon Tall Tower Observatory (ATTO). Atmos. Res. 327, 108351. https://doi.org/10.1016/j.atmosres.2025.108351.

Oliveira, P.E.S., Acevedo, O.C., Sörgel, M., Tsokankunku, A., Wolff, S., Araújo, A.C., Souza, R.A.F., Sá, M.O., Manzi, A.O., Andreae, M.O., 2018. Nighttime wind and scalar variability within and above an Amazonian canopy. Atmos. Chem. Phys. 18, 3083–3099. https://doi.org/10.5194/acp-18-3083-2018.

Peel, M.C., Finlayson, B.L., McMahon, T.A., 2007. Updated world map of the Köppen-Geiger climate classification. Hydrol. Earth Syst. Sci. 11, 1633–1644. https://doi.org/10.5194/hess-11-1633-2007.

Peterson, C.J., Ribeiro, G.H.P., de, M., Negrón-Juárez, R., Marra, D.M., Chambers, J.Q., Higuchi, N., Lima, A., Cannon, J.B., 2019. Critical wind speeds suggest wind could be an important disturbance agent in Amazonian forests. For. An Int. J. For. Res. *92*, 444-459,. https://doi.org/10.1093/forestry/cpz025.

Phillips, O.L., Vásquez Martínez, R., Monteagudo Mendoza, A., Baker, T.R., Núñez Vargas, P., 2005. LARGE LIANAS AS HYPERDYNAMIC ELEMENTS OF THE TROPICAL FOREST CANOPY. Ecology 86, 1250–1258. https://doi.org/10.1890/04-1446.

Pinto, A.C., Higuchi, N., Iida, S., Santos, J., Ribeiro, R.J., Rocha, R.M., Silva, R.P., 2003. Padrão de distribuição espacial de espécies florestais que ocorrem na região de Manaus. Higuchi et al. (Ed.). Projeto Jacaranda Fase II - Pesquisas Florestais Na Amazônia Central. Editado Por HIGUCHI et Al.). Manaus, AM, pp. 1–20.

Podobnik, B., Stanley, H.E., 2008. Detrended Cross-Correlation Analysis: A New Method for Analyzing Two Nonstationary Time Series. Phys. Rev. Lett. 100, 084102. https://doi.org/10.1103/PhysRevLett.100.084102.

Quine, C.P., Gardiner, B.A., Moore, J., 2021. Wind disturbance in forests: The process of wind created gaps, tree overturning, and stem breakage. Plant Disturbance Ecology. Elsevier, pp. 117–184. https://doi.org/10.1016/B978-0-12-818813-2.00004-6.

R Core Team, 2025. R: A language and environment for statistical computing. R Foundation for Statistical Computing.

Rehbein, A., Ambrizzi, T., 2023. Mesoscale convective systems over the Amazon basin in a changing climate under global warming. Clim. Dyn. 61, 1815–1827. https://doi.org/10.1007/s00382-022-06657-8.

Rehbein, A., Ambrizzi, T., Mechoso, C.R., 2018. Mesoscale convective systems over the Amazon basin. Part I: climatological aspects. Int. J. Climatol. 38, 215–229. https://doi.org/10.1002/joc.5171.

Rehbein, A., Ambrizzi, T., Mechoso, C.R., Espinosa, S.A.I., Myers, T.A., 2019. Mesoscale convective systems over the Amazon basin: The GoAmazon2014/5 program. Int. J. Climatol. *39*, 5599-5618,. https://doi.org/10.1002/joc.6173.

Rennó, C.D., Nobre, A.D., Cuartas, L.A., Soares, J.V., Hodnett, M.G., Tomasella, J., Waterloo, M.J., 2008. HAND, a new terrain descriptor using SRTM-DEM: Mapping terra-firme rainforest environments in Amazonia. Remote Sens. Environ. 112, 3469–3481. https://doi.org/10.1016/j.rse.2008.03.018.

Ribeiro, G.H.P.M., Chambers, J.Q., Peterson, C.J., Trumbore, S.E., Magnabosco Marra, D., Wirth, C., Cannon, J.B., Négron-Juárez, R.I., Lima, A.J.N., de Paula, E.V.C. M., Santos, J., Higuchi, N., 2016. Mechanical vulnerability and resistance to snapping and uprooting for Central Amazon tree species. For. Ecol. Manage. *380*, 1-10,. https://doi.org/10.1016/j.foreco.2016.08.039.

Rifai, S.W., Urquiza Muñoz, J.D., Negrón-Juárez, R.I., Ramírez Arévalo, F.R., Tello-Espinoza, R., Vanderwel, M.C., Lichstein, J.W., Chambers, J.Q., Bohlman, S.A., 2016. Landscape-scale consequences of differential tree mortality from catastrophic wind disturbance in the Amazon. Ecol. Appl. *26*, 2225-2237,. https://doi.org/10.1002/eap.1368.

Rollenbeck, R., Trachte, K., Bendix, J., 2016. A New Class of Quality Controls for Micrometeorological Data in Complex Tropical Environments. J. Atmos. Ocean. Technol. 33, 169–183. https://doi.org/10.1175/JTECH-D-15-0062.1.

Ruel, J.C., Pin, D., Cooper, K., 1998. Effect of topography on wind behaviour in a complex terrain. Forestry *71*, 261-265,. https://doi.org/10.1093/forestry/71.3.261.

Ruel, J.C., Pin, D., Cooper, K., 2001. Windthrow in riparian buffer strips: Effect of wind exposure, thinning and strip width. Forest Ecology and Management *143*, 105-113,. https://doi.org/10.1016/S0378-1127(00)00510-7.

Santana, R.A., Dias-Júnior, C.Q., da Silva, J.T., Fuentes, J.D., do Vale, R.S., Alves, E.G., dos Santos, R.M.N., Manzi, A.O., 2018. Air turbulence characteristics at multiple sites in and above the Amazon rainforest canopy. Agric. For. Meteorol. 260-261, 41–54. https://doi.org/10.1016/J.AGRFORMET.2018.05.027.

Schmitt, A.U., Ament, F., de Araújo, A.C., Sá, M., Teixeira, P., 2023. Modeling atmosphere–land interactions at a rainforest site – a case study using Amazon Tall Tower Observatory (ATTO) measurements and reanalysis data. Atmos. Chem. Phys. 23, 9323–9346. https://doi.org/10.5194/acp-23-9323-2023.

Segura, H., Espinoza, J.C., Junquas, C., Lebel, T., Vuille, M., Garreaud, R., 2020. Recent changes in the precipitation-driving processes over the southern tropical Andes/western Amazon. Clim. Dyn. 54, 2613–2631. https://doi.org/10.1007/s00382-020-05132-6.

Silva Dias, M.A.F., 2002. Cloud and rain processes in a biosphere-atmosphere interaction context in the Amazon Region. J. Geophys. Res. 107, 8072. https://doi.org/10.1029/2001JD000335.

Simonetti, A., Araujo, R.F., Celes, C.H.S., da Silva e Silva, F.R., dos Santos, J., Higuchi, N., Trumbore, S., Magnabosco Marra, D., 2023. Canopy gaps and associated losses of biomass – combining UAV imagery and field data in a central Amazon forest. Biogeosciences 20, 3651–3666. https://doi.org/10.5194/bg-20-3651-2023.

Sombroek, W., 2001. Spatial and Temporal Patterns of Amazon Rainfall. AMBIO A J. Hum. Environ. 30, 388–396. https://doi.org/10.1579/0044-7447-30.7.388.

Telles, E., de, C.C., de Camargo, P.B., Martinelli, L.A., Trumbore, S.E., da Costa, E.S., Santos, J., Higuchi, N., Oliveira, R.C., 2003. Influence of soil texture on carbon dynamics and storage potential in tropical forest soils of Amazonia. Global Biogeochem. Cycles 17. https://doi.org/10.1029/2002gb001953 n/a-n/a.

Tóta, J., Roy Fitzjarrald, D., Da Silva Dias, M.A.F., 2012. Amazon rainforest exchange of carbon and subcanopy air flow: Manaus LBA SiteA complex terrain condition. Sci. World J. *2012*, 1-19,. https://doi.org/10.1100/2012/165067.

Urquiza Muñoz, J.D., Magnabosco Marra, D., Negrón-Juarez, R.I., Tello-Espinoza, R., Alegría-Muñoz, W., Pacheco-Gómez, T., Rifai, S.W., Chambers, J.Q., Jenkins, H.S., Brenning, A., Trumbore, S.E., 2021. Recovery of Forest Structure Following Large-Scale Windthrows in the Northwestern Amazon. Forests 12, 667. https://doi.org/10.3390/f12060667.

Urquiza-Muñoz, J.D., Trumbore, S., Negrón-Juárez, R.I., Feng, Y., Brenning, A., Vasquez-Parana, C.M., Marra, D.M., 2024. Increased Occurrence of Large-Scale Windthrows Across the Amazon Basin. AGU Adv 5. https://doi.org/10.1029/2023AV001030.

Van Emmerik, T., Steele-Dunne, S., Gentine, P., Oliveira, R.S., Bittencourt, P., Barros, F., Van De Giesen, N., 2018. Ideas and perspectives: Tree-atmosphere interaction responds to water-related stem variations. Biogeosciences 15, 6439–6449. https://doi.org/10.5194/bg-15-6439-2018.

van Emmerik, T., Steele-Dunne, S., Guerin, M., Gentine, P., Oliveira, R., Hut, R., Selker, J., Wagner, J., van de Giesen, N., 2018. Tree Sway Time Series of 7 Amazon Tree Species (July 2015–May 2016). Front. Earth Sci. 6, 411456. https://doi.org/10.3389/feart.2018.00221.

Van Emmerik, T., Steele-Dunne, S., Hut, R., Gentine, P., Guerin, M., Oliveira, R.S., Wagner, J., Selker, J., Van De Giesen, N., 2017. Measuring tree properties and responses using low-cost accelerometers. Sensors (Switzerland) *17*, 1098,. https://doi.org/10.3390/s17051098.

Vickers, D., Mahrt, L., 1997. Quality Control and Flux Sampling Problems for Tower and Aircraft Data. J. Atmos. Ocean. Technol. 14, 512–526. https://doi.org/10.1175/1520-0426(1997)014<0512:QCAFSP>2.0.CO;2.

Wakimoto, R.M., 1985. Forecasting Dry Microburst Activity over the High Plains. Mon. Weather Rev. 113, 1131–1143. https://doi.org/10.1175/1520-0493(1985)113<1131:FDMAOT>2.0.CO;2.

Wang, W., Chen, F., 2025. Wind Field Modeling over Hilly Terrain: A Review of Methods, Challenges, Limitations, and Future Directions. Appl. Sci. 15, 10186. https://doi.org/10.3390/app151810186.

Williams, E., Rosenfeld, D., Madden, N., Gerlach, J., Gears, N., Atkinson, L., Dunnemann, N., Frostrom, G., Antonio, M., Biazon, B., Camargo, R., Franca, H., Gomes, A., Lima, M., Machado, R., Manhaes, S., Nachtigall, L., Piva, H., Quintiliano, W., Machado, L., Artaxo, P., Roberts, G., Renno, N., Blakeslee, R., Bailey, J., Boccippio, D., Betts, A., Wolff, D., Roy, B., Halverson, J., Rickenbach, T., Fuentes, J., Avelino, E., 2002. Contrasting convective regimes over the Amazon: Implications for cloud electrification. J. Geophys. Res. Atmos. 107, 50–51. https://doi.org/10.1029/2001JD000380. LBA.

Zahn, E., Chor, T.L., Dias, N.L., 2016. A simple methodology for quality control of micrometeorological datasets. Am J Env. Eng 6, 135–142. https://doi.org/10.5923/s.ajee.201601.20.

Zebende, G.F., 2011. DCCA cross-correlation coefficient: Quantifying level of cross-correlation. Phys. A Stat. Mech. its Appl. 390, 614–618. https://doi.org/10.1016/j.physa.2010.10.022.

Zhuang, Y., Fu, R., Marengo, J.A., Wang, H., 2017. Seasonal variation of shallow-to-deep convection transition and its link to the environmental conditions over the Central Amazon. J. Geophys. Res. *122*, 2649-2666,. https://doi.org/10.1002/2016JD025993.